Petrology, Vol. 10, No. 6, 2002, pp. 495–518. Translated from Petrologiya, Vol. 10, No. 6, 2002, pp. 563–588.

Geochemical Thermometry of the Layered Series Rocks of the Skaergaard Intrusion

A. A. Ariskin

Vernadsky Institute of Geochemistry and Analytical Chemistry, Russian Academy of Sciences, ul. Kosygina 19, Moscow, 119991 Russia
e-mail: ariskin@geokhi.ru

Received April 23, 2002

Abstract—Using the COMAGMAT-3.65 (2000) program, we modeled the equilibrium crystallization of melts that correspond to the 65 rock compositions representing the main zones of the Layered Series of the Skaergaard intrusion. The computation at P = 1 kbar and the conditions closed with respect to oxygen allowed us to estimate the intervals of temperatures (1145–1085°C) and oxygen fugacities (from QFM + 1 to 1.5 log units in the Lower Zone to QFM and even lower in the Upper Zone) typical of magmas, from which the Skaergaard cumulates have crystallized. The compositions of the residual (intercumulus) melts were also calculated. They are characterized by strong enrichment in FeO* (up to ~18 wt %) and TiO_2 (up to ~5.5 wt %) with insignificant variations of SiO_2 contents (48–50 wt %). These compositions plotted in the OLIV–CPX–QTZ diagram indicate that the major part of the Layered Series crystallized within the stability field of the *Ol–Pl–Cpx* cotectic and Fe–Ti oxides. Some small differences are found in the compositions of the intercumulus melts for the LZa/LZb and LZc/MZ/UZa intervals, which cannot be explained only by fractional crystallization. These differences are within the computation accuracy at temperatures of about 1100°C. However, they may be caused by the infiltration processes, including migration and re-equilibration of interstitial liquid. The compositions obtained by L.R. Wager using the mass-balance calculations are located in this diagram too far from the experimental line of the *Ol–Pl–Cpx* equilibrium to be a real approximation for the low-pressure evolution of the Skaergaard magma. The main problem of genetic interpretation of the Skaergaard intrusion is the misbalance between the weighted average composition of the intrusion and the parental magma composition. The TiO_2 and P_2O_5 misbalance is most pronounced: the concentrations of these components are several times higher than those in any proposed parental magma. These discrepancies could partially be related to heterogeneity of the Skaergaard magma, which entrained large amount of *Ol* and *Pl* crystals to the intrusive magma chamber. However, we believe that the significant volume of ilmenite–magnetite gabbro could not originate without the formation of complementary more silicic material, even if some amount of troctolite cumulates is suggested to exist at a depth.

INTRODUCTION

The results of study of the Skaergaard intrusion significantly advanced the igneous petrology. For many petrologists, this intrusion is a kind of a natural laboratory and a classical example of perfect fractionation of basaltic magma under the closed conditions. Excellent exposure, weak weathering degree, detailed sampling, and distinct geologic relationships between the main structural units of the intrusion make it an appropriate object for development and testing of various petrologic concepts and approaches. That is why the methods of interpretation of the chemical composition and structure of rocks first tried for the Skaergaard intrusion more than 60 years ago are the important instruments in studies of large layered complexes and differentiated sills.

In the late 1930s, Wager and Deer proposed a simple graphic procedure for estimating the evolution of the chemical composition of the Skaergaard magma during the intrusive magma chamber differentiation (Wager and Deer, 1939; Wager, 1960). This approach was based on three premises: (1) the parental magma is devoid of crystal phases, (2) the volumes of the parental magma derivatives are proportional to the thicknesses of the corresponding zones of the Layered Series in the central part of the intrusion, and (3) the composition of the Skaergaard magma is approximated by the sample EG4507 from the Marginal Border Series.

According to these data (Wager and Brown, 1967), the compositional series calculated for system crystallinity (F) between 0 and 88% composes a monotonous trend with increasing total iron (FeO*) approximately from 9.5 to 18 wt % with SiO_2 decrease from 48 to 47 wt %. The final crystallization stages are characterized by a small enrichment in FeO* with SiO_2 increase up to 50 wt %, which is followed by a decrease of the iron oxide concentrations and the formation of unusual ferroandesite compositions: at F = 99.3%, FeO* and SiO_2 concentrations in the model differentiates are 18.5 and 55.0 wt %, respectively (Fig. 1). The calculated trend became a standard for the tholeiitic magma evolution with the maximum enrichment in iron and was

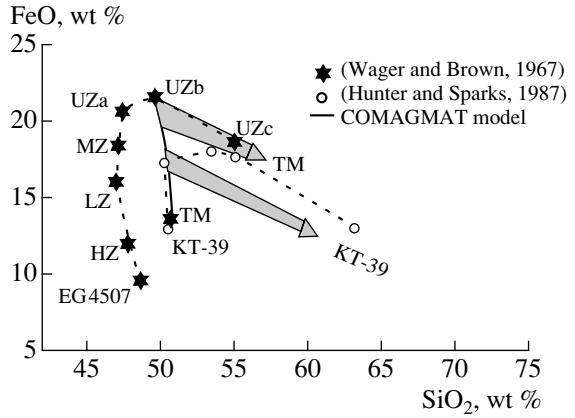

Fig. 1. Trends of the Skaergaard magma differentiation.
Natural rock trends are based on the results of mass-balance calculations for individual zones of the Layered Series (Wager and Brown, 1967; Hunter and Sparks, 1987): HZ, Hidden Zone (after 35% crystallization of the parental magma); LZ, Lower Zone (76%); MZ, Middle Zone (88.2%). The Upper Zone comprises three subzones: UZa (95.7%), UZb (98.2%), and UZc (99.3%) Crystallization trends shown by arrows are obtained by modeling using the COMAGMAT-3.5 program at P = 1 atm and redox condition of the QFM buffer (Ariskin, 1999). TM is the initial composition at 1165°C calculated by geochemical thermometry of contact rocks from the Marginal Border Series (Table 1); EG4507 and KT-39 are the chilled gabbro samples (Wager and Brown, 1967; Hoover, 1989).

expressed in the compositions of some dikes associated with the Skaergaard intrusion (Brooks and Nielsen, 1978, 1990). This trend was repeated by mass-balance calculations for the Kiglapait intrusion in Labrador (Morse, 1981).

The further studies revealed some weak points in the Wager's approach. Firstly, the intrusion of the overheated homogenous melt into the chamber is hardly possible from the physical viewpoint. The calculations of the intrusion dynamics under the nonisothermal conditions demonstrate that the basaltic magma filling the funnel-shaped chambers can contain from 10–15 to 40% crystal phases in relation to the rate of magma influx and cooling degree (Sharapov *et al.*, 1997). Secondly, the mass balance during the graphical reconstructions required the assumption that a significant part of the intrusion is not exposed, so-called Hidden Layered Series (Wager, 1960); however, it is not verified by the geophysical data (Blank and Gettings, 1973). Finally, there are some reasons to believe that the chilled gabbro EG4507 was contaminated by host rocks and cannot be used as a model for the initial melt (McBirney, 1975; Hoover, 1989).

Moreover, the exclusion of the Upper and Border Marginal Series from the calculation and using only the volumes of the rocks of the Layered Series could introduce some additional errors, because the volumetric proportions of the three main units of the Skaergaard intrusion are comparable (McBirney, 1996). These observations require a cautious consideration of the estimates made by Wager and its colleagues, but are not in conflict with the probable magma evolution of the Skaergaard intrusion to the rocks with high iron contents. It is obvious that revealing the trends of compositional evolution of magmatic melts should not only meet the mass-balance condition, but also be consistent with the principles of phase equilibria and crystallization laws for the basaltic systems, if the element partitioning in the melt–crystal system was assumed to be the main factor of magma fractionation. In this context, the classical evolutionary trend of the Skaergaard magma seems to be controversial (Fig. 1).

Hunter and Sparks (1987) noted that the trend with strong enrichment in iron at monotonous decrease of SiO_2 contents is inconsistent with the estimated composition of the parental Skaergaard magma (Wager, 1960; Wager and Brown, 1967). This concerns both the iron enrichment degree and the trend with the SiO_2 decrease, which does not correspond to 44–46 wt % SiO_2 in the crystallization products of the gabbro association, while the sample EG4507 contains >48 wt % SiO_2. Another inconsistency with the experimental data is that the calculated bend of the evolutionary trend and the transition to the SiO_2 increase in the residual liquid do not coincide with the onset of the titanomagnetite crystallization. The latter early appears in the succession of the rocks of the Layered Series, at the stage of SiO_2 depletion in the model differentiates and monotonous iron enrichment (Wager and Brown, 1967). It was suggested that the differentiation of the Skaergaard magma actually exemplifies the evolution of the tholeiitic magma from ferrobasalt to basaltic andesite and icelandite (ferroandesite) typical of the volcanic series. The main difference between the actual chemical evolution of the Skaergaard magma and the evolution of the typical tholeiitic series is the elevated, but not anomalous, degree of iron enrichment caused by reduced conditions in the magma chamber (Hunter and Sparks, 1987). This consideration was verified by mass-balance calculations based on the method of subtraction of the gabbroic components from the composition of the chilled gabbro KT-39 (Fig. 1, Table 1), which is believed to better approximate the composition of the initial magma of the Skaergaard intrusion (Hoover, 1989).

The new interpretation has not met a positive response among the petrologists, who mapped the rock relationships of the intrusion (McBirney and Naslund, 1990; Brooks and Nielsen, 1990). It was generally because of the Hunter and Sparks's calculations produced large amounts of intermediate and silicic derivatives, which contradicted the comprehensive data on the structure of the Skaergaard intrusion. It is worthy noting that the trend of the gradual enrichment in FeO* is consistent with the plagioclase compositions, which show monotonous iron enrichment upsection the Layered Series (Tegner, 1997). High iron enrichment in the residual magmas of the Skaergaard intrusion is indi-

Table 1. Compositions of chilled gabbro and initial compositions for the rocks of the Marginal Border Series compared to the weighted average composition of the Skaergaard intrusion

Oxides	Chilled gabbro of the Marginal Border Series		Compositions of the initial intercumulus melts		Average composition of the intrusion
	EG4507	KT-39	EC-22	TM	
SiO_2	48.58	50.46	51.30	49.94	46.26
TiO_2	1.18	2.70	1.61	1.68	4.22
Al_2O_3	17.40	13.41	12.99	12.93	12.40
FeO*	9.73	12.96	13.55	13.22	17.26
MnO	0.16	0.22	0.26	0.19	0.27
MgO	8.71	6.71	6.13	6.89	6.29
CaO	11.50	10.34	11.15	12.38	10.07
Na_2O	2.39	2.41	2.37	2.37	2.40
K_2O	0.25	0.57	0.28	0.26	0.36
P_2O_5	0.10	0.22	0.09	0.15	0.45

Note: Samples from the Marginal Border Series: EG4507 (Wager and Brown, 1967), KT-39 (Hoover, 1989). Initial melts: EC-22 is experimental glass obtained by melting of a contact rock sample at 1160°C under the QFM buffer conditions (Hoover, 1989); TM is average of six model liquids by the geochemical thermometry data for contact cumulates at 1165°C (Ariskin, 1999). Weighted average composition of the intrusion is calculated by A. McBirney (personal communication) and is based on the average compositions of the Layered Series (LS), Upper Border Series (UBS), and Marginal Border Series (MBS) with their volume proportions assumed to be LS/UBS/MBS = 50/20/30. All compositions are normalized to 100%.

rectly justified by the occurrence of granophyre segregations composing up to 15% of the rocks of the Sandwich Horizon. According to the experimental and geochemical data, granophyres could be produced by liquid immiscibility of basic magma highly enriched in FeO* (McBirney and Nakamura, 1973; McBirney, 1975).

However, the opponents of this new interpretation did not solve the problem of inconsistency between the classical trend proposed by Wager and the data on phase equilibria in the ferrobasaltic systems (Hunter and Sparks, 1990; Ariskin, 1998). Moreover, the conclusions of Hunter and Sparks (1987) agreed with the main results of computer modeling of fractional crystallization of the Skaergaard magma (Ariskin *et al.*, 1987; Toplis and Carroll, 1996; Ariskin, 1999).

Modeling of Fractional Crystallization

The first calculations of fractionation of the EG4507 composition were performed using the TOLEMAG program (Ariskin *et al.*, 1987), preceding the COMAGMAT computer model (Ariskin *et al.*, 1993; Ariskin and Barmina, 2000). The calculations for the systems closed and open (IW–QFM) with respect to oxygen were carried out for 1 atm pressure and dry conditions. These calculations adequately reproduced the cumulate sequence in the Layered Series: $Ol + Pl \longrightarrow Ol + Pl + Aug \longrightarrow Ol + Pl + Aug + Mt \pm Pig$, except for *Ilm*, which appeared only under the most reduced, IW buffer conditions. However, regardless of the redox conditions, all of the model trends showed significant enrichment of melt in SiO_2 at the initial crystallization stage of the *Ol* + *Pl* assemblage approximately up to 50 wt % SiO_2, i. e., up to the inflexion point corresponding to the onset of the augite crystallization. Further fractionation resulted in some depletion of melt in SiO_2 and its enrichment in iron (up to 15–18 wt % FeO*), which terminated by the appearance of Fe and Ti oxides on the liquidus. The magnetite (±*Ilm*) separation was accompanied by the formation of ferroandesites close to icelandites of Thingmuli volcano (Carmichael, 1964). Similar results were obtained later by using a semiempirical model based on the experimentally studied phase relations for a synthetic starting material, which approximated the composition of a dike comagmatic to the Skaergaard intrusion (Toplis and Carroll, 1995, 1996).

The calculation performed with a modified version of the program, COMAGMAT-3.5 (Ariskin, 1999) using more realistic models of *Mt* and *Ilm* crystallization (Ariskin and Barmina, 1999), justified our previous results, i. e., no of the model evolutionary lines reproduces the Wager's trend (Fig. 1). It was found again that the magnetite crystallization in the systems buffered with respect to oxygen lead to strong depletion of melt in iron and its enrichment in SiO_2, while FeO* contents slightly decrease in the closed systems. More detailed consideration of these differences can be found in the corresponding sections of the book (Ariskin and Barmina, 2000). Let us make the main conclusions of the computer modeling of the fractional crystallization of the Skaergaard magma:

(1) The results of our calculations indicate a rather insignificant and short-term depletion of the residual melts in SiO_2 after the appearance of high-Ca clinopy-

roxene at the crystallization stage of the *Ol–Pl–Aug* assemblage.

(2) The *Mt* separation causes SiO_2 accumulation in melt in the systems both open and closed with respect to oxygen.

(3) The highest degree of iron enrichment in the residual liquids ranges from 18 to 20 wt % for different initial melt compositions and does not exceed 22 wt % FeO*.

The Experimental Determination of the Trapped Melt Composition

The above examples of calculation of lines of the Skaergaard magma fractional crystallization belong to the methods of direct modeling of the geochemical processes. These methods require presetting some initial composition and possible P–T–f_{O_2} conditions of fractionation of a parental melt. As an alternative or, more precisely, as the amendment and verification criterion for these approaches, one can use some other methods of genetic interpretation solving the reverse petrologic–geochemical problems. When applied to the problems related to the layered intrusions, they are based on the suggestion that the interstices among the cumulus minerals or primocrysts are always filled with trapped liquid. The compositions of this liquid can approximate the evolution of the main magma volume. This suggestion assumes that the system was completely closed after the cumulus formation, i.e., the migration or reequilibration of the interstitial liquid do not occur. Properly speaking, this condition should be proved for each sample. However, it is also possible that the bulk rock composition actually is a record of proportions and chemistry not only of the cumulative phases, but also of the *initial* intergranular liquid. There are the experimental and numerical methods for estimating its composition.

The experimental approach consists of partial melting of rocks by their exposure to the above-solidus temperatures and subsequent study of the glass compositions in the interstices of the relict mineral grains assumed to be primary mineral crystals. McBirney and Nakamura (1973) performed a series of such experiments with gabbroids from the main zones of the Layered Series of the Skaergaard intrusion. They found that, at temperatures <1150°C and redox conditions corresponding to the WM–QFM buffers, the residual melts are strongly enriched in iron and depleted in SiO_2 (McBirney and Naslund, 1990), i. e., the main features of the Wager's trend was reproduced. Some additional experiments were carried out with the contact gabbro samples from the Marginal Border Series (Hoover, 1989). The glasses obtained by the melting of these least evolved rocks at 1160–1180°C under the QFM buffer conditions had notably higher SiO_2 and lower FeO* contents as compared to the residual melts in experiments with the rocks of the Layered Series (Fig. 2). According to our data, these compositional differences can be partly related to temperature differences during experimental melting (Ariskin, 1999).

The latter result exemplifies the main difficulties of the experimental approach: without knowledge of the temperature of equilibrium between the primary crystals and melt, the researcher risks to obtain during the interpretation of the experimental data the compositions that significantly deviate from the initial characteristics. This is most probable during the consideration of multiphase magnetite-bearing assemblages at a melting degree below 50%, when long run duration is necessary to approach the equilibrium in the melt–crystal system and between Fe^{3+} and Fe^{2+} in the liquid phase. However, the magnetite–ilmenite gabbroids were the main objects in the study of McBirney and Nakamura (1973).

Some examples of solution of the reverse problem for the Skaergaard rocks using the methods of computer modeling of phase equilibria in the basaltic system will be considered below. This approach called the "method of geochemical thermometry" (Frenkel' *et al.*, 1987) cannot offer an alternative to the experimental studies and has certain application limits. However, it allows a reliable estimation of temperatures of the initial crystal + melt mixtures and reduces the range of probable compositions of the trapped liquids.

GEOCHEMICAL THERMOMETRY OF THE SKAERGAARD ROCKS

The thermodynamic parameters of the intrusive rock formation include pressure, temperature, redox conditions, initial composition of the trapped liquids, compositions of primary crystals, and relative proportions of cumulus phases and intergranular liquid. If the pressure and redox conditions are known (estimated by independent methods), the rest of the above parameters can be determined by solving a reverse problem using a modeling of primary crystal–melt equilibria for individual samples or rock groups with similar compositions of interstitial liquids. These calculations are carried out with a COMAGMAT computer model in a certain sequence depending on the study objective (Ariskin and Barmina, 2000). The study of the origin of the intrusive basic rocks is typically aimed at estimating the composition and crystallinity of the initial magma, the proportions of cumulus minerals at various stages of differentiation (or within the neighboring rhythms), and some other parameters related to the dynamics of the magma chamber crystallization. Regardless of the petrologic goals, the calculation is subdivided into several stages: (1) selection of samples for calculations, (2) numerical experiments on equilibrium crystallization of melts approximated by the rock compositions, (3) derivation of the temperature–concentration dependencies for the model liquids, and (4) search for the region of intersection of the evolutionary lines, which corresponds to the temperature of primary equilibrium

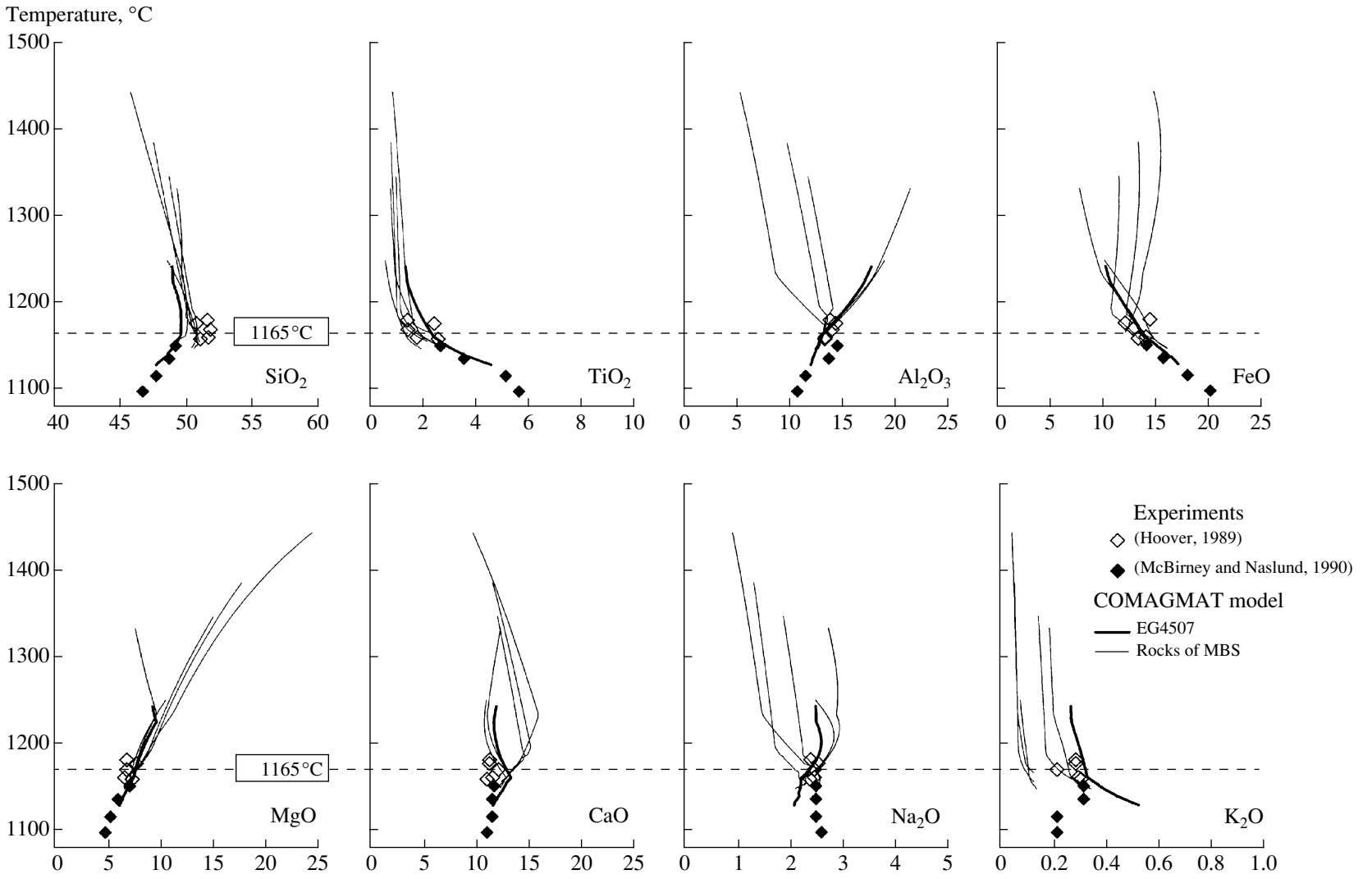

Fig. 2. Results of experimental study of the intercumulus melt composition in the Skaergaard rocks and data of geochemical thermometry of contact cumulates from the Marginal Border Series.

Results of quenching experiments for the rocks of the Marginal Border Series (Hoover, 1989) and the Lower Zone of the Layered Series (McBirney and Nakamura, 1973; McBirney and Naslund, 1990). Lines represent the trajectories of equilibrium crystallization of melts for the chilled gabbro EG4507 and samples UT-04, UT-08, EC-10, MEO-10, and KT-47 calculated by the program COMAGMAT-3.5 (Ariskin, 1999). Temperature of 1165 ± 10°C was assumed to be the initial temperature for the Skaergaard magma.

between melt and crystals and to the intergranular melt composition. These procedures were termed "geochemical thermometry" emphasizing the primary importance of the temperature estimation (Frenkel' *et al.*, 1987).

A series of previous publications was devoted to the reconstruction of the temperature–composition dependencies and phase characteristics of the initial magmas for the low-evolved traps of the Siberian Platform (Frenkel' *et al.*, 1988; Ariskin and Barmina, 2000), the eastern Kamchatka sills (Barmina *et al.*, 1989), the Partridge River and Talnakh intrusions (Chalokwu *et al.*, 1993; Krivolutskaya *et al.*, 2001), and several large intrusions, namely, Skaergaard, Kiglapait, and Dovyren (Ariskin, 1999; Ariskin *et al.*, 2002; Barmina and Ariskin, 2002). In this paper, we consider the results of the thermodynamic calculations aimed at the determination of the chemical evolution of residual melts during the Skaergaard magma chamber crystallization.

Method Description

The method of geochemical thermometry of rocks along the vertical section of a differentiated igneous body and estimation of the compositional evolution of the initial magma during its fractionation were first tested for the case of the Vel'minskii dolerite sill (Frenkel' *et al.*, 1987; Barmina *et al.*, 1988). Our approach in the present study is based on the hypothesis that, regardless of the accepted differentiation mechanism (directional crystallization or crystal settling), the major rock masses form from floor upward, which suggests the directed, regular variations in the compositions of melt and minerals crystallizing from the main magma volume. As a consequence, for each rock, the average composition of the overlying part of the intrusion corresponds to the bulk composition of the crystal + melt mixture (i. e., magma), from which this rock has crystallized. The differences between the compositions of rock and residual magma at each level can be related with variations in relative proportions of minerals and liquid, rather than their compositions. As it follows from the previous sections, such a data set is a perfect object for geochemical thermometry.

The procedure comprises in this case the numerical modeling of the trajectories for equilibrium crystallization of a pair of initial compositions. One of them corresponds to the bulk rock composition at this level, while the other, to the weighted average composition of the overlying part of the intrusion. The intersection point of these trajectories in the composition–temperature space determines the conditions of the rock formation, phase composition of the magma, and some chemical features of the melt, from which the minerals of this rock have crystallized. As applied to the relatively thin sills, this approach was found to be highly informative and easy in use (Frenkel' *et al.*, 1988; Ariskin and Barmina, 2000). Unfortunately, this approach cannot be used for large intrusions, because most of the layered intrusions have a complex lateral structure, and the data on the typical and representative sections cannot be extrapolated to the whole volume of the intrusion.

There is a version of geochemical thermometry that can be used without the data on the bulk composition of the magma, from which the rock has crystallized. Several compositionally different samples characterizing a rather thin interval of the vertical section or a key horizon can be used for calculations. It could be suggested that these bulk compositions "record" the information on the composition of the same residual (trapped) liquid and equilibrium mineral assemblage. Then, the search for the region of the trajectory intersection becomes reasonable, and the composition of the residual melt within this interval (horizon) can be calculated as the average of several compositions of model liquids at the specified temperature of the initial equilibrium. A single difference (and drawback) of this version is that the phase composition of the residual magma (the proportions of crystals at various differentiation stages) cannot be determined, because of the absence of model trajectory for the bulk composition of this magma. Thus, for the temperature calculation along a given vertical section (no matter, real or generalized) one should first classify the available analyses into several groups, for which similar compositions of residual liquids can be implied. The data on the Skaergaard intrusion can be reliably subdivided into such groups.

The Intrusion Structure and Sample Selection

The Skaergaard layered intrusion of basic rocks $\sim 6 \times 11$ km in the map view is situated on the eastern coast of Greenland (Fig. 3). The intrusion forms a cube-shaped funnel tilted to the south and has an exposed thickness of about 3.5 km. A part of the intrusion is not exposed. It is the so-called Hidden Layered Series, which probably does not exceed 10–15% of the intrusion volume (McBirney, 1989). The main units of the Skaergaard intrusion (Fig. 4) are the Layered Series (LS) and the overlying Upper Border Series (UBS). Their volume proportion is about 2 : 1 (Wager and Deer, 1939). The Marginal Border Series (MBS) rims the intrusion along its contacts with host rocks and also is an important structural unit (Fig. 3). The Layered Series is a rock sequence formed upward from the floor of the intrusive magma chamber. It differs structurally and lithologically from the MBS and UBS, which crystallized inward the intrusion from its walls and roof. The upper boundary of the Layered Series corresponds to its contact with the Upper Border Series along a certain level known as the Sandwich Horizon (SH) (Wager and Deer, 1939). It is easily mapped by the abrupt transition from mesocratic ferrodiorites of the Layered Series to more felsic rocks of the UBS (McBirney, 1989).

The scheme of subdivision of the Layered Series into zones differing in cumulus mineralogy is based on the Wager and Brown's nomenclature (Wager and

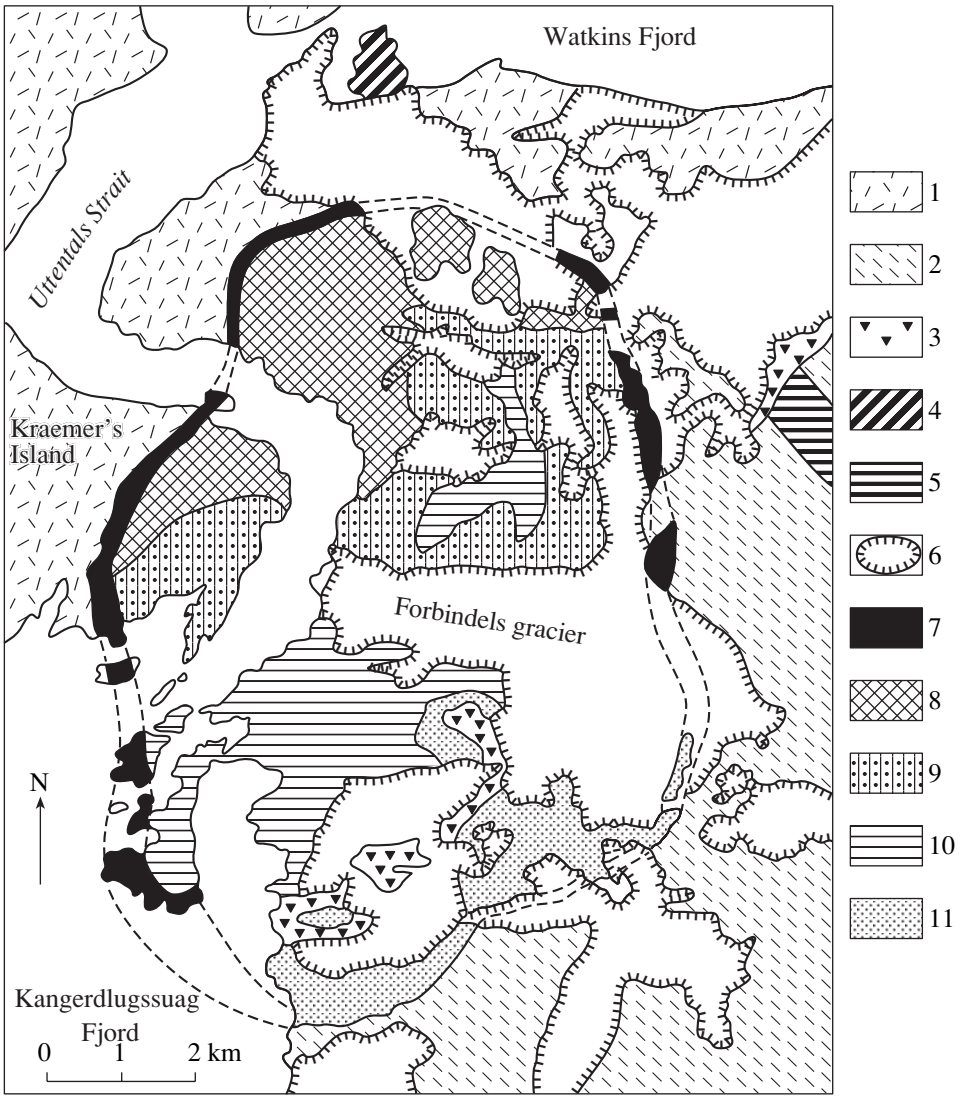

Fig. 3. A scheme of geologic relationships between the rocks of the Marginal Border Series and the main structural units of the Skaergaard intrusion, after (McBirney, 1996).

(1) Precambrian gneisses; (2) Tertiary basalts; (3) individual intrusive bodies; (4) peridotite; (5) sedimentary rocks; (6) glaciers and snow. Skaergaard intrusion: (7) Marginal Border Series; (8–10) Layered Series with the Lower (8), Middle (9), and Upper (10) zones; (11) Upper Border Series.

Brown, 1967). The zones are shown in Fig. 4 according to (McBirney, 1996). The Layered Series is subdivided into the Lower (LZ), Middle (MZ), and Upper (UZ) zones. Their contacts are determined by disappearance of cumulate olivine at the base of the Middle Zone and its reappearance in the rocks of the Upper Zone. Actually, *Ol* occurs in the rocks of the MZ as rare grains and thin reaction rims between pyroxenes and Fe–Ti oxides. This observation is important for interpretation of the computer modeling results. The Lower Zone of the Layered Series is divided into three subzones (LZa, LZb, and LZc) by poikilitic pyroxene texture in the LZa and by the increase of oxide content (*Ilm* + *Mt*) at the base of the LZc. The Upper Zone also consists of three subzones (UZa, UZb, and UZc) distinguished by abundant apatite in the UZb and mosaic inverted ferrobustamite in the UZc. The inverted *Pig* occurs in small amount in the Upper Zone up to the middle of the UZa. The upper part of the Upper Zone includes interstitial granophyre.

Sample selection. Sixty five rock samples representing five zones from the LZa to UZa (Fig. 4) were selected for geochemical thermometry. The sample location and their geochemical features are given in (McBirney, 1998). A single modification concerns sample LB-238, which is affiliated with the LZa, rather than with the LZb. The most differentiated rocks of the UZb, UZc, and SH are excluded from our calculation, because the apatite crystallization does not considered

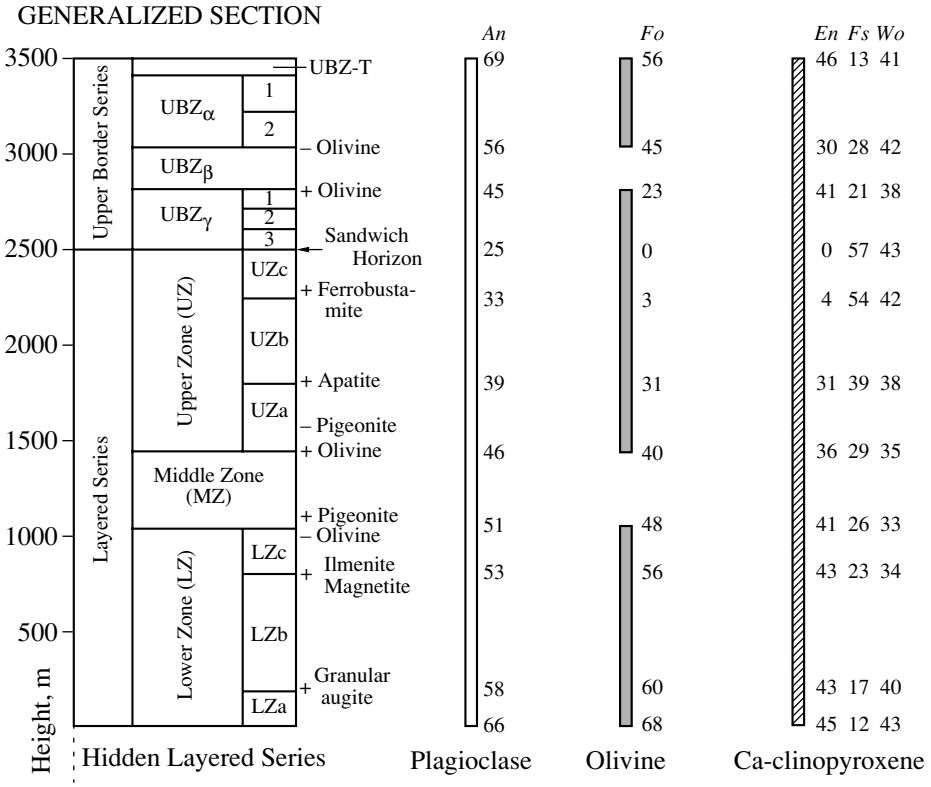

Fig. 4. The main structural units of the Layered Series and the Upper Border Series with compositional evolution of the rock-forming minerals (McBirney, 1996).

Zones of the Layered Series are distinguished by the appearance and disappearance of some primary cumulus minerals or by transition from rocks with poikilitic clinopyroxene to those with granular clinopyroxene (for LZb). The Upper Border Series is subdivided into three subzones (α, β, and γ) equivalent to the units of the Upper Zone (UZ) in the Layered Series. The *Ol*, *Pl*, and *Aug* compositions shown at the boundaries of individual zones are approximate and can slightly vary along the boundaries.

yet in our model. Moreover, five average compositions of the main units of the Layered Series and their five equivalents from the Marginal Border Series (Table 2) were used for testing and controlling calculations. The data previously obtained in geochemical thermometry of six contact rocks from the Marginal Border Series (Ariskin, 1999; Ariskin and Barmina, 2000) were involved for interpretation of the computer modeling results.

Crystallization Conditions and Preliminary Calculations

Estimation of intervals of the intensive parameters during crystallization and evolution of the Skaergaard magma are important for further calculations. The relationships of silica polymorphs and ferrous pyroxenes in the rocks of the Sandwich Horizon gave the crystallization pressure (600 ± 100 bar) and temperature (970 ± 20°C) at this level (Lindsley *et al.*, 1969). According to the density of the overlying gabbroids and basalts, these conditions correspond to the depth of 2 km for the Sandwich Horizon and 4.5–3.0 km from the surface for the lower parts of the LZa and UZa horizons (McBirney, 1996). This means that the Lower Zone of the Layered Series began to crystallize at about 1.5 kbar, while the boundary between the Middle and Upper zones corresponds to pressures of about 0.9 kbar.

The estimation of the redox conditions of the Skaergaard magma crystallization is based on the analysis of the mineral equilibria (Lindsley *et al.*, 1969; Williams, 1971; Morse *et al.*, 1980; Frost *et al.*, 1988; Frost and Lindsley, 1992) and the data of electrochemical measurements (Sato and Valenza, 1980; Kersting *et al.*, 1989). The thermodynamic calculations show similar results, according to which the oxygen fugacity at the base of the LZa subzone was some higher than QFM (Williams, 1971; Morse *et al.*, 1980; Frost and Lindsley, 1992) and gradually decreased to the Middle Zone. Within the Upper Zone, the f_{O_2} strongly decreased up to the values corresponding to QFM – 2 in the rocks of the Sandwich Horizon (Frost *et al.*, 1988). These estimations do not contradict the phase relations in the rocks of the Layered Series for the interval of WM–QFM buffers (McBirney and Nakamura, 1973; McBirney and Naslund, 1990). The measurements of the intrinsic oxygen fugacity in the rocks indicate higher fugacity values covering the interval from about IW–

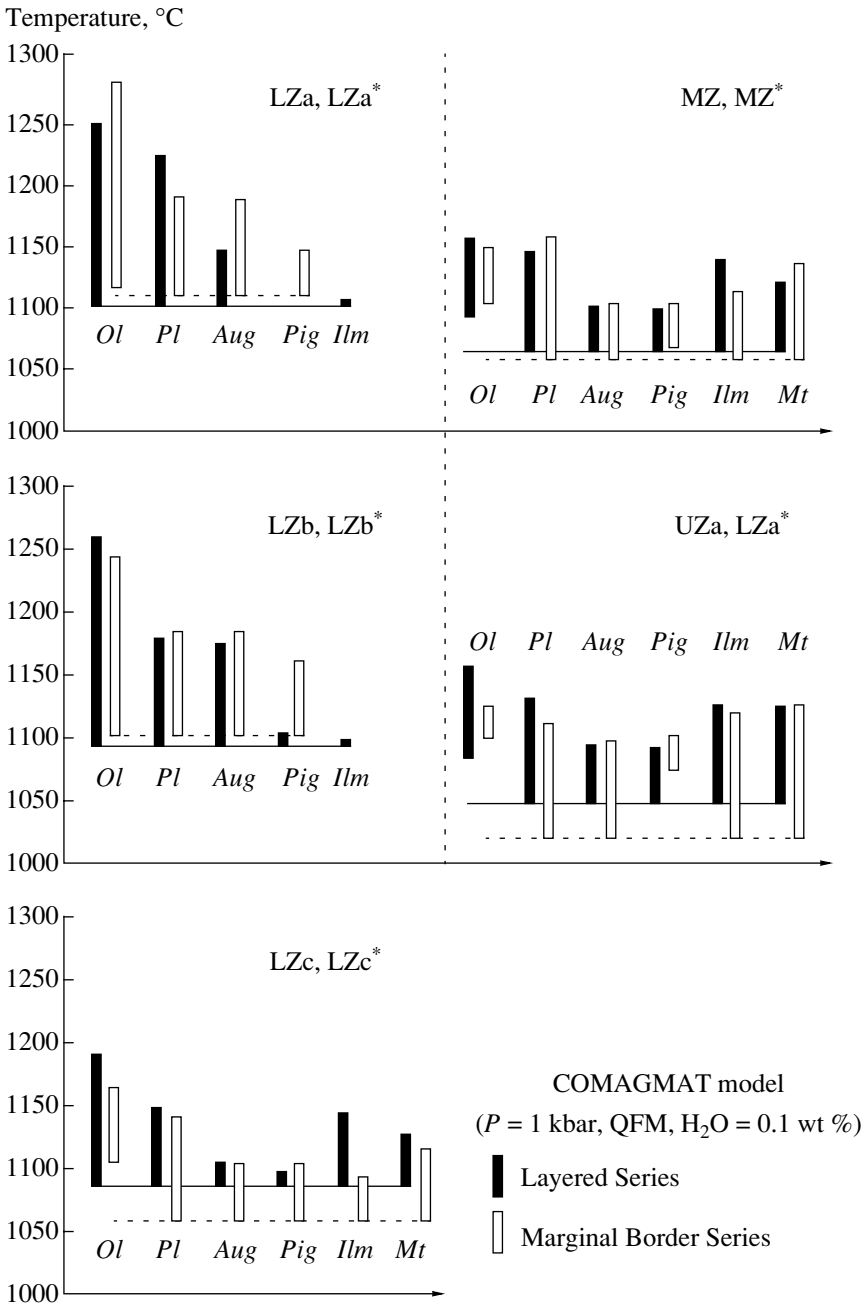

Fig. 5. Sequences of mineral crystallization calculated for average compositions of the main zones of the Layered Series and their equivalents from the Marginal Border Series (Table 2).

Calculation of equilibrium crystallization was performed using the COMAGMAT-3.65 program at P = 1 kbar, 0.1 wt % H_2O in the initial system, and redox conditions of the QFM buffer.

WM (Sato and Valenza, 1980) to QFM + 0.5 to 1.5 logarithmic units (Kersting *et al.*, 1989).

Based on the mineral compositions in the *Ol–Pig–Mt–Ilm* assemblages from the LZc, MZ, and UZa, Williams (1971) calculated the temperatures of "frozen" equilibria within the interval of 1150–1050°C. The highest temperatures are typical of the rocks of the Lower Zone. These values are consistent with the previous estimates for the Sandwich Horizon (970°C) and correspond to the temperature range of experimental melting (1150–1002°C), which yielded the glasses approximating the residual melts for the rocks of the Layered Series (McBirney and Naslund, 1990). The experimental results for the chilled gabbro KT-39 (Hoover, 1989) and data on geochemical thermometry of the contact rocks (Ariskin, 1999) indicate that the highest temperature of the Skaergaard magma crystallization did not exceed 1165°C, which corresponds to

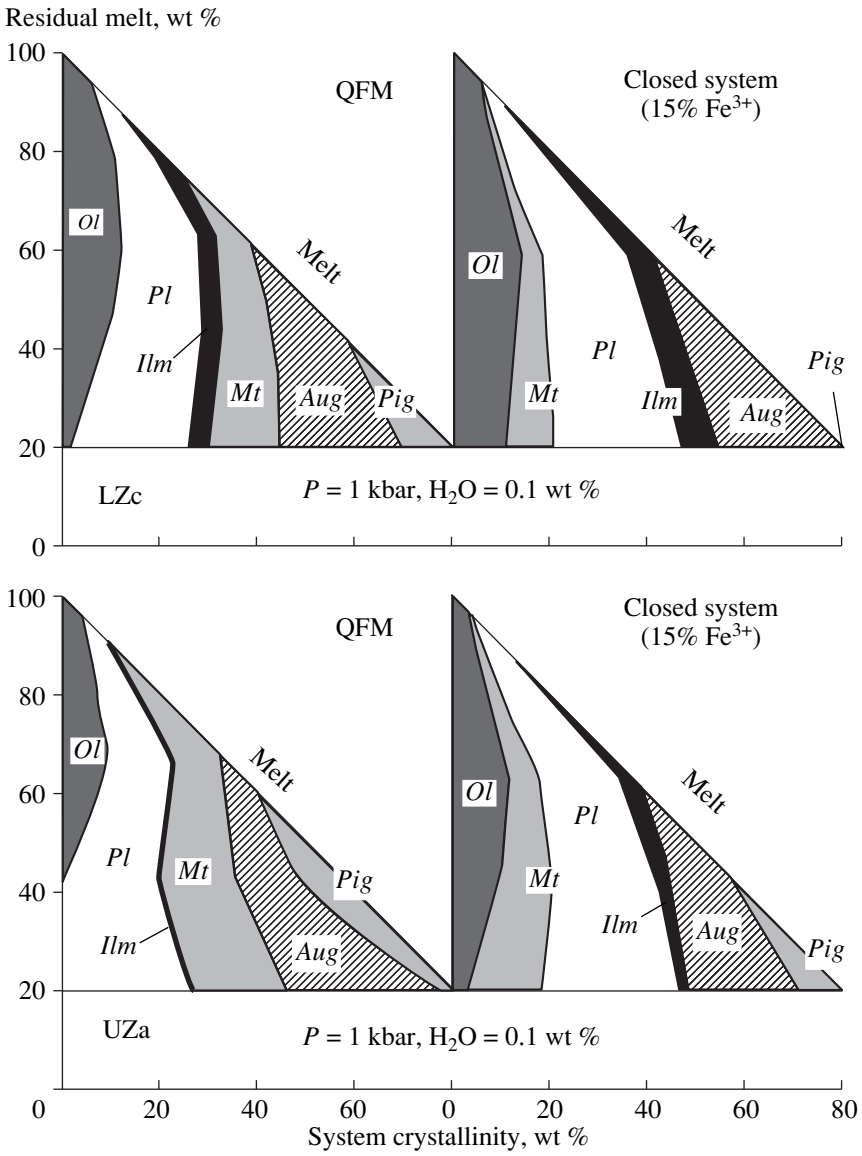

Fig. 6. The evolution of phase proportions during the magma crystallization for the average compositions of the LZc and UZa rocks (Table 2).
Calculation of equilibrium crystallization was performed using the COMAGMAT-3.65 program at P = 1 kbar, 0.1 wt % H_2O in the initial system; open systems are characterized by the redox conditions of the QFM buffer; closed systems have a fixed $Fe^{3+}/(Fe^{3+} + Fe^{2+})$ ratio of 0.15 in melt.

the olivine and plagioclase crystallization at the liquidus. The temperature values obtained by bimineral equilibria (oxides, pyroxene) are too high, probably because of the subsolidus re-equilibration (Jang and Naslund, 2001).

Thus, the petrologic studies allowed the estimation of the whole range of intensive parameters of the Skaergaard magma crystallization. Its fractionation began at about 1.5 kbar and ~1165°C under the QFM buffer conditions and proceeded with decreasing pressure, temperature, and oxygen fugacity (McBirney, 1996).

Modeling of Phase Equilibria for the Average Compositions

The reliability of the further temperature calculations can be verified and some mineralogic features of the Skaergaard rocks can be revealed by computer modeling of crystallization of the melts corresponding to the average compositions of the main zones of the Layered Series (Figs. 5, 6). The calculations were performed at P = 1 kbar for the systems closed and open (from QFM + 1 to QFM – 2) with respect to oxygen. The water content in the system was accepted to be

Table 2. Average compositions of the main zones of the Layered Series and their equivalents from the Marginal Border Series (McBirney, 1996)

Oxides	LS	MBS	LS	MBS	LS	MBS	LS	MBS	LS	MBS
	LZa	LZa*	LZb	LZb*	LZc	LZc*	MZ	MZ*	UZa	UZa*
SiO_2	48.12	49.43	48.84	50.30	41.10	44.86	42.79	43.46	43.07	44.33
TiO_2	1.35	1.00	1.44	1.08	6.92	4.91	6.79	5.44	5.67	6.24
Al_2O_3	16.81	13.71	12.55	14.13	11.02	11.35	11.53	12.48	11.17	10.05
FeO*	11.13	11.87	12.84	11.83	21.10	19.02	20.00	20.51	22.52	21.47
MnO	0.16	0.19	0.21	0.18	0.26	0.26	0.26	0.23	0.31	0.29
MgO	9.42	10.77	10.13	9.42	7.61	6.60	6.24	5.64	5.62	5.57
CaO	10.11	10.76	11.57	10.89	9.77	10.59	9.87	9.54	8.62	9.39
Na_2O	2.52	1.93	2.13	1.88	1.97	2.03	2.23	2.24	2.55	2.08
K_2O	0.27	0.25	0.20	0.22	0.20	0.26	0.21	0.35	0.26	0.34
P_2O_5	0.11	0.08	0.09	0.07	0.05	0.13	0.08	0.12	0.22	0.24

Note: LS, Layered Series; MBS, Marginal Border Series. All compositions are normalized to 100 wt %.

0.1 wt %. A new COMAGMAT model (version 3.65, 2000) was used. It was calibrated for the iron-rich systems with liquidus temperatures at about 1100°C.[1]

Figure 5 shows the results of calculation of equilibrium crystallization under the conditions of the QFM buffer for average compositions of the five subzones of the Layered Series (LZa, LZb, LZc, MZ, and UZa) and their equivalents from the Marginal Border Series (LZa*, LZb*, LZc*, MZ*, and UZa*) (Table 2). The calculations reached the 80% crystallinity of the system (or 20% interstitial liquid). The data demonstrate some common features and certain differences. In general, the sequences of mineral crystallization are consistent in the rocks of the compared horizons, which justifies the formation of both compositional groups from the same magma. For example, a small field of single *Ol* crystallization is observed for the LZa and LZb compositions, which is followed by *Pl* and *Aug* crystallization. The field of clinopyroxene crystallization significantly expands in the LZb rocks, which correlates with crystallization of abundant granular augite. The LZc trajectories show early *Ilm* and *Mt* crystallization, which is consistent with the mineralogic composition of rocks in this zone (Fig. 4). Similar relationships are found for the rocks of the Middle and Upper zones; however, olivine completely dissolves here by reaction with residual liquid.

The pigeonite crystallization also has some specific features. This mineral crystallizes earlier in the rocks of the Marginal Border Series than in the Layered Series; its early crystallization is accompanied by early dissolution of olivine. This correlates with higher SiO_2 contents in the MBS (Table 2) and could indicate some small, but principal, differences between the compositions of the interstitial materials in the rocks of the Marginal Border Series and Layered Series (Ariskin, 1999). Apparently, these features explain the lower temperatures of the MBS mineral assemblages at a high crystallinity of average compositions (Fig. 5). As to the gabbroids enriched in oxides, ilmenite and magnetite begin to crystallize almost simultaneously in both rock groups (from LZc to UZa and from LZc* to UZa*), although *Ilm* begins to crystallize some earlier than *Mt* in the Layered Series. Thus, the results of calculation for the QFM conditions (Fig. 5) are compatible with the general scheme of the intrusion structure. The model *Ol* behavior in the rocks of the Upper Zone is an exception.

A complete dissolution of *Ol* at the final stages suggests that this mineral must be absent within the Middle Zone and in the more evolved rocks of the Upper Zone. Meanwhile, the reappearance of olivine is the main petrographic criterion for separation of the MZ from the UZa (Wager and Deer, 1939; McBirney, 1989, 1996). In order to avoid the contradiction within the frame of the crystallization mechanisms, we performed a series of additional calculations modeling crystallization of

[1] The main problems in application of the COMAGMAT-3.5 program (Ariskin and Barmina, 1999) to the rocks of the Layered Series are related to low temperatures of mineral assemblages in the LZc, MZ, and UZa, typically ~1115–1080°C (McBirney, 1996). These temperatures are significantly lower than the experimental temperatures of 1120–1350°C used in the model for calibration of equations for equilibria of *Ol*, *Pl*, and pyroxenes. As a result, the calculations by means of the COMAGMAT-3.5 program led to a shift of phase boundaries at temperatures below 1100°C and, consequently, to an unreasonable expansion of the *Aug* stability field at the expense of the *Pl* and *Pig* fields. That is why, we have revised and enlarged the experimental database to increase the amount of experiments at temperatures ≤1100°C. This work and corresponding re-equilibration was carried out using the INFOREX database (Ariskin and Barmina, 2000), while new mineral–melt geothermometers for mafic minerals and plagioclase composed the empirical basis for the COMAGMAT-3.65 model. Testing of this program using the data of independent experiments increased insignificantly the accuracy of the temperature calculations, while the *Pl* composition and phase relations between *Aug* and *Pig* became much more realistic.

the average compositions of zones of the Layered Series under the conditions closed with respect to oxygen. The crystallization trajectories were calculated at P = 1 kbar, 0.1 wt % water, and various ferric to ferrous iron ratios in the system: 0.1 ≤ FE3# ≤ 0.25, where FE3# = $Fe^{3+}/(Fe^{3+} + Fe^{2+})$. The main results are shown in Fig. 6. They comprise the analysis of variations of mineral proportions during the closed system crystallization as compared to the data calculated at the QFM buffer conditions. The proportion of mineral phases is shown in these diagrams as a function of the residual liquid amount (or system crystallinity).

Proportions of Olivine and Oxides

The modeling results for the closed system show a significant expansion of the *Ol* stability field. For example, 4–10% *Ol* crystallizes at the liquidus in the rock of the LZc and UZa up to the system crystallinity of about 80% (Fig. 6). Such a behavior is related to the reduction of the *Pig* crystallization field and correlates with a decrease of total oxide content as compared to the data for the QFM buffered system. Thus, the decrease of the oxide proportion in the closed system results in slower SiO_2 enrichment in the melt. This effect reduces the field of pigeonite crystallization and hampers complete dissolution of olivine. Thus, the problem of "disappearance" and "reappearance" of *Ol* in the crystallization sequence is attributed to the peritectic reaction of the following type: $Ol + l \longrightarrow Aug\ (\pm Pig) + Mt\ (\pm Ilm) \pm Pl$. We observed such relationships in the computer modeling results since the middle 1980s. We considered them to be artifacts related to the imperfect model of magnetite crystallization (Ariskin *et al.*, 1987). The calculations based on new, more precise geothermometers for *Ilm* and *Mt* (Ariskin and Barmina, 1999) indicate that this peritectic reaction actually occurs in the ferrobasaltic systems. The reaction relationships among olivine, pyroxenes, and Fe–Ti oxides are observed in thin sections of the rocks of the Skaergaard intrusion (McBirney, 1996).

It is also interesting that the *Pig* field is notably wider for the UZa composition than for the UZc composition (Fig. 6). This correlates with elevated SiO_2 contents in the rocks of the Upper Border Series (compare average SiO_2 contents of ~43.1 and 41.1 wt %, Table 2), in spite of the systematically higher total iron contents in these rocks (~22.5 wt % FeO* against 21.1 wt % in the UZc). This fact may indicate that the trapped melt in the rocks of the Upper Border Series had higher silica activity as compared to the rocks of the Lower Zone of the Layered Series. This preliminary result does not agree with the Wager's trend (Fig. 1), but is verified by later results of the thermometric calculations. However, it should be taken into account that the observed appearance of *Ol* in the rocks of the UZa is accompanied by *Pig* disappearance at the same level as a result of the increasing amount of the interstitial granophyre (McBirney, 1996).

The obtained data on proportions of Fe–Ti oxides are also very important. The calculations with the COMAGMAT-3.65 program show that the amount of *Mt* crystallizing in the closed system is about two thirds of the *Mt* amount crystallizing under the conditions buffered with respect to oxygen. This phenomenon was demonstrated in experiments (Osborn, 1959; Presnall, 1966) and verified by modeling of phase equilibria (Ghiorso and Carmichael, 1985; Ariskin *et al.*, 1987; Toplis and Carroll, 1996; Ariskin and Barmina, 2000). New data concern the ilmenite crystallization. In the closed system, the *Ilm* proportion and its ratio to *Mt* increase (Fig. 6). Thus, we could imply that the Skaergaard magma crystallized as a closed system, because the ilmenite predominates over magnetite in the rocks of the Layered Series (McBirney, 1989). The nearly coeval crystallization of *Ilm* and *Mt* obtained in our calculations is consistent with experimental data (Snyder *et al.*, 1993). These authors demonstrated that the ilmenite crystallization in the closed system decreases the FeO concentration in the liquid, thus increasing the Fe^{3+}/Fe^{2+} ratio and stabilizing the occurrence of the iron oxides. In contrast, the *Mt* crystallization decreases the Fe_2O_3 concentration and increases the reduction degree of the melt. As a result, the composition migrates to the field of *Ilm* stability. Thus, mutually compensating effects of crystallization of different Fe–Ti oxides operate in the iron- and titanium-rich systems (including the Skaergaard melts). These effects are expressed in a convergence of stability fields of these minerals at nearly equal temperatures of their appearance.

Some Conclusions

The modeling of equilibrium crystallization of the initial compositions corresponding to the average compositions of the main zones of the Layered Series and the Marginal Border Series demonstrated that the version 3.65 of the COMAGMAT computer model allows us to predict the phase equilibria in the Skaergaard rocks, including complex relationships among the residual melt, *Ol*, *Aug*, *Pig*, *Ilm*, and *Mt*. It is found that the equilibrium proportions of silicate minerals and Fe–Ti oxides strongly depend on the redox conditions determining the direction of the residual liquid evolution.

The early *Mt* crystallization and high contents of iron oxides in the crystal phases are expected for the Skaergaard rocks at elevated oxygen fugacity (>QFM). These processes cause the SiO_2 enrichment and complementary FeO* depletion in melt. The SiO_2 increase leads to peritectic dissolution of *Ol* within the field of high-Ca pyroxene and magnetite crystallization. The *Ol* dissolution is accelerated by *Pig* appearance. The expansion of the *Pig* stability field is a typical feature of phase evolution of the ferrobasaltic systems during the oxide crystallization and is accompanied by increase of silica activity and deceleration of the Mg/(Mg + Fe) decrease in the liquid. The early olivine can be com-

pletely dissolved at the final crystallization stages, which is exemplified by the rock compositions in the Middle and Upper zones of the Layered Series (Fig. 5). At the oxygen fugacities of the QFM buffer and lower values, *Ilm* can crystallize earlier than *Mt*, and SiO_2 accumulation becomes less significant. In this case, *Pig* crystallizes some later, and the field of *Ol* stability within the interval of peritectic reaction increases.

The *Ol* and *Pig* proportions during crystallization of the systems closed with respect to oxygen depend on the oxidation degree, which can be related with the evolution of the $Fe^{3+}/(Fe^{3+} + Fe^{2+})$ ratio in melt. High FE3# values stabilize *Pig*, because of the larger amount of the crystallizing *Mt* and higher degree of SiO_2 enrichment. The removal of Fe_2O_3 with magnetite is accompanied by the melt reduction and expansion of the ilmenite stability field (Fig. 6). The main effect of the closed system is expressed in a decrease of total proportion of oxides among the crystallizing phases at a moderate SiO_2 increase and FeO* decrease in the residual liquid.

The results of modeling of the phase equilibria indicate that the domination of *Ilm* over *Mt* typical of the LZc rocks can occur only in the closed system. The conditions closed with respect to oxygen (or open with respect to a reducing agent; see below) should be also suggested for the rocks of the Upper Zone of the Layered Series, because these conditions can stabilize *Ol* and preserve it from complete dissolution at the final stages of the rock crystallization. Note, however, that these conclusions are valid only for the oxidized rocks (Fig. 6) with initial FE3# = 0.15, which corresponds to the oxygen fugacity slightly below the NNO buffer value. According to the above data, the rocks of the Skaergaard intrusion had a rather low oxidation degree of the residual melt, and *Ol* can be stabilized relative to *Pig* at the later crystallization stages.

Modeling of the Formation Conditions for the Rocks of the Layered Series

Unlike the calculations for some other intrusive bodies (Frenkel' *et al.*, 1988; Chalokwu *et al.*, 1993; Krivolutskaya *et al.*, 2001; Barmina and Ariskin, 2002; Ariskin *et al.*, 2002), the oxygen fugacity has not been preset in the geochemical thermometry of the layered rocks of the Skaergaard intrusion. The calculations by the COMAGMAT 3.65 program used the observed FeO and Fe_2O_3 concentrations and calculated FE3# values for each sample (the data were graciously provided by Prof. A. McBirney, Oregon University, USA). This suggests an ideally closed system and probable overestimation of the iron oxidation degree due to the rock weathering. However, the samples are fresh and devoid of distinct evidence of secondary alteration (McBirney, 1998). Such an approach allows the oxygen fugacity estimation in the initial melt by the solution of a reverse problem, i. e., calculation of the f_{O_2} values at known temperature and the residual melt composition (Nikolaev *et al.*, 1996). Summarizing the data for individual zones of the Layered Series, we can trace the general evolution of the oxygen fugacity during the Skaergaard magma differentiation. Thus, the geochemical thermometry was applied to 65 initial compositions with a given FE3# ratio for each rock. Each studied zone was characterized by several samples: $n = 8$ for LZa, $n = 16$ for LZb, $n = 11$ for LZc, $n = 20$ for MZ, and $n = 10$ for UZa. The pressure differences between these zones do not exceed 0.6 kbar (see above) and do not notably effect the calculation accuracy under the isobaric conditions at $P = 1$ kbar and primary magmatic water concentration of 0.1 wt %. The crystallization increment was 1 mol %. The calculations were stopped, when the system crystallinity of 75–80% had been reached.

The LZa subzone. A wide range of liquidus temperatures was found within the field of *Ol* crystallization by computer modeling for five initial compositions with MgO > 9.5 wt %. Olivine was followed by *Pl* and *Aug* and, then, by *Mt* and *Pig*. These relationships can be presented by the following sequence: *Ol* (1322–1258°C) ⟶ *Pl* (1237–1193°C) ⟶ *Aug* ± *Mt* (1140–1110°C) ⟶ *Pig* (1125–1110°C). Early *Pl* and *Aug* crystallization was observed in the Ca richest sample LB-238 (~12.6 wt % CaO): *Pl* (1230°C) ⟶ *Ol* (1196°C) ⟶ *Aug* (1181°C) ⟶ *Mt* + *Pig* (1120–1110°C), while sample LA-753 demonstrated the subcotectic relationships: *Ol* + *Pl* (1210–1200°C) ⟶ *Aug* (1153°C) ⟶ *Mt* + *Pig* (1125–1115°C). The *Ilm* crystallization (fractions of percent) was observed in three cases at <1110°C. Titanomagnetite was first to crystallize at 1190°C only in one sample LA-347 enriched in oxides (5.8 wt % TiO_2 and 18.3 wt % FeO*). Except for the samples LA-347 and LA-753, the calculated lines of descent form a single group of six cotectics closely converging within the temperature range of 1140–1150°C. This fact allows us to consider the primary assemblages of these rocks as mechanical mixtures of olivine and plagioclase crystals with interstitial liquid. The average composition of this cluster at 1145°C is given in Table 3 and shown in Fig. 7 together with the calculation data for the LZb subzone. The average compositions of *Ol* and *Pl* for six samples at 1145°C are $Fo_{74.9 \pm 1.5}$ and $An_{66.3 \pm 1.9}$. The *An* content in plagioclase is generally consistent with the natural compositions (Fig. 4). The model *Ol* composition is by about 7 mol % more magnesian than the natural compositions. However, this discrepancy cannot be attributed to the calculation errors of the COMAGMAT program, which calculates the *Ol* compositions with an accuracy of to 1–2% *Fo* (Ariskin and Barmina, 2000). It is more probable that the elevated iron proportion in the natural mineral is caused by re-equilibration of primary *Ol* crystals by their reaction with the FeO-rich residual melt.

As was reported above, the calculation by this program allows one to estimate the evolution of the intrinsic oxygen fugacity in the melt. This evolution is caused by changes in the Fe^{3+}/Fe^{2+} ratio in the residual

liquid during the crystallization of mafic silicate minerals and oxides. The $\log f_{O_2}$ values are estimated for each temperature using the parameters from (Sack *et al.*, 1980) with an accuracy of about ±1 (Nikolaev *et al.*, 1996). The model *T*–$\log f_{O_2}$ trajectories for the ideally closed systems should intersect, like in the temperature–concentration diagrams (Fig. 2). Then, the average $\log f_{O_2}$ values for several trajectories at a known temperature of the primary equilibrium characterizes the redox conditions, at which the initial cumulus mineral assemblage has formed. Our calculation gave $\log f_{O_2} = -7.5 \pm 0.6$ for the rocks of the LZa at 1145°C. This value is about 1.5 logarithmic units higher than the QFM buffer value and is consistent with the measured values (Kersting *et al.*, 1989). This result is shown in Fig. 7 together with estimate for the rocks of the overlying horizon.

The LZb subzone. Three main types of model sequences are determined for this subzone. Four compositions showed the sequence of *Ol* (1370–1240°C) ⟶ *Pl* (1220–1170°C) ⟶ *Aug* ± *Mt* (1160–1110°C) ⟶ *Pig* (<1130°C). In five cases, *Aug* appeared at 1200–1170°C together with *Ol* or closely after it. Plagioclase was the first mineral to crystallize at 1250–1190°C in seven samples. Titanomagnetite typically was fourth to crystallize, and *Pig* and *Ilm* were found only at the later stages at temperatures below ~1120 and 1100°C, respectively. These calculations are consistent with petrologic observations indicating changes in textural features and abundance of augite in the LZb and do not contradict the conclusion that *Aug* crystallized and accumulated there as the third cotectic phase, together with *Ol* and *Pl* (Wager and Brown, 1967; McBirney, 1989). The evolutionary lines of the melt compositions form a distinct convergence at temperatures below 1140°C: the most dense cluster of the intersecting trajectories roughly corresponds to 1125 ± 5°C (Fig. 7, Table 3). The calculated average compositions of minerals at this temperature are $An_{61.9 \pm 2.1}$ and $Fo_{72.1 \pm 2.1}$. The plagioclase composition is similar to the natural data within the frames of the applied model for the *Pl*–liquid equilibrium (Ariskin and Barmina, 2000). The composition of model *Ol* even more strongly deviates from the natural composition (by 12–16 mol % *Fo*). We believe that this deviation is related to decreasing content of modal *Ol* and increasing degree of its subsolidus re-equilibration. The calculated *Aug* composition is also more magnesian, but the deviation from the natural composition is not so large (Fig. 4, Table 3). The average oxygen fugacity during the formation of the LZb rocks was estimated at $\log f_{O_2} = -7.4 \pm 0.7$ (Fig. 7).

The LZc subzone. As compared to the rocks of the LZa and LZb, the modeling of crystallization of the LZc rock compositions gave an even larger diversity in the sequences of mineral crystallization. This is related to a larger abundance of oxides. For example, *Ilm* and *Mt* were first to crystallize at 1270–1170°C in six cases. The sequence of crystallization of the silicate phases varied (*Ol* ⟶ *Pl* ⟶ *Aug* + *Pig* or *Ol* ⟶ *Aug* + *Pig* ⟶ *Pl*) and pyroxenes have never been observed at temperatures >1110°C. This temperature is accepted to be the highest stability limit of the primary assemblage of *Ol* + *Pl* + *Aug* + *Mt* + *Ilm*. Olivine crystallized before the other minerals in three cases, plagioclase was first to crystallize in one case (at 1203°C), and a subcotectic assemblage of *Ol* + *Pl* is found at 1157°C for one sample. These data verify the conclusion that Fe–Ti oxides are primary cumulus phases in the LZc (Wager and Brown, 1967). The estimation of the trapped liquid compositions for these rocks is more real when the crystallization sequence and *Mt* and *Ilm* proportions determining the SiO_2 and FeO* covariations in the residual melt are correctly predicted. The modal mineralogy, including Fe–Ti oxides, was previously determined for all of the eleven magnetite–ilmenite gabbro samples from LZc (McBirney, 1998). Some of these data are compared with the results of thermometric calculations in Table 4. It is seen that the COMAGMAT-3.65 model rather correctly predicts the bulk proportions of magnetite and ilmenite after the model rock crystallization. This fact substantiates the reliability of the calculated lines of the residual melt evolution (Fig. 8).

The model trajectories of the LZc rocks form an intersection at about 1100°C. The corresponding melts are slightly depleted in SiO_2 and enriched in TiO_2 and FeO* as compared to the interstitial liquid for the underlying LZb (compare their average compositions from Table 3). Note that the Al_2O_3 and MgO concentrations in the LZc melts continue to decrease due to the fractionation laws, while a notable increase of CaO concentrations is observed. This behavior can hardly be interpreted within the model of fractional crystallization with simultaneous separation of plagioclase and high-Ca pyroxene. Possible explanation of this fact will be presented below. Note that the CaO content decreases within the uncertainty interval of the geochemical thermometry (see standard deviations for CaO concentrations in melt in Table 3). The initial compositions of *Ol*, *Pl*, and pyroxenes in equilibrium with the LZc melt correspond to general tendency of depletion in refractory components upsection the intrusive chamber. The model compositions of *Ilm* and *Mt* are shown in Table 3 as $FeTiO_3$ and Fe_2TiO_4 activities calculated by the method of (Stormer, 1983). These compositions correspond to the nearly stoichiometric ilmenite and titanomagnetite with moderate iron content, which are consistent with the shift of the redox conditions of the primary equilibrium to lower oxygen fugacities (QFM, Fig. 8).

The Middle Zone. Twenty samples are used for geochemical thermometry of the Middle Zone (McBirney, 1998). The variations of the initial compositions and oxidation degrees of the rocks determine various crystallization sequences, where six minerals (*Ol*, *Pl*,

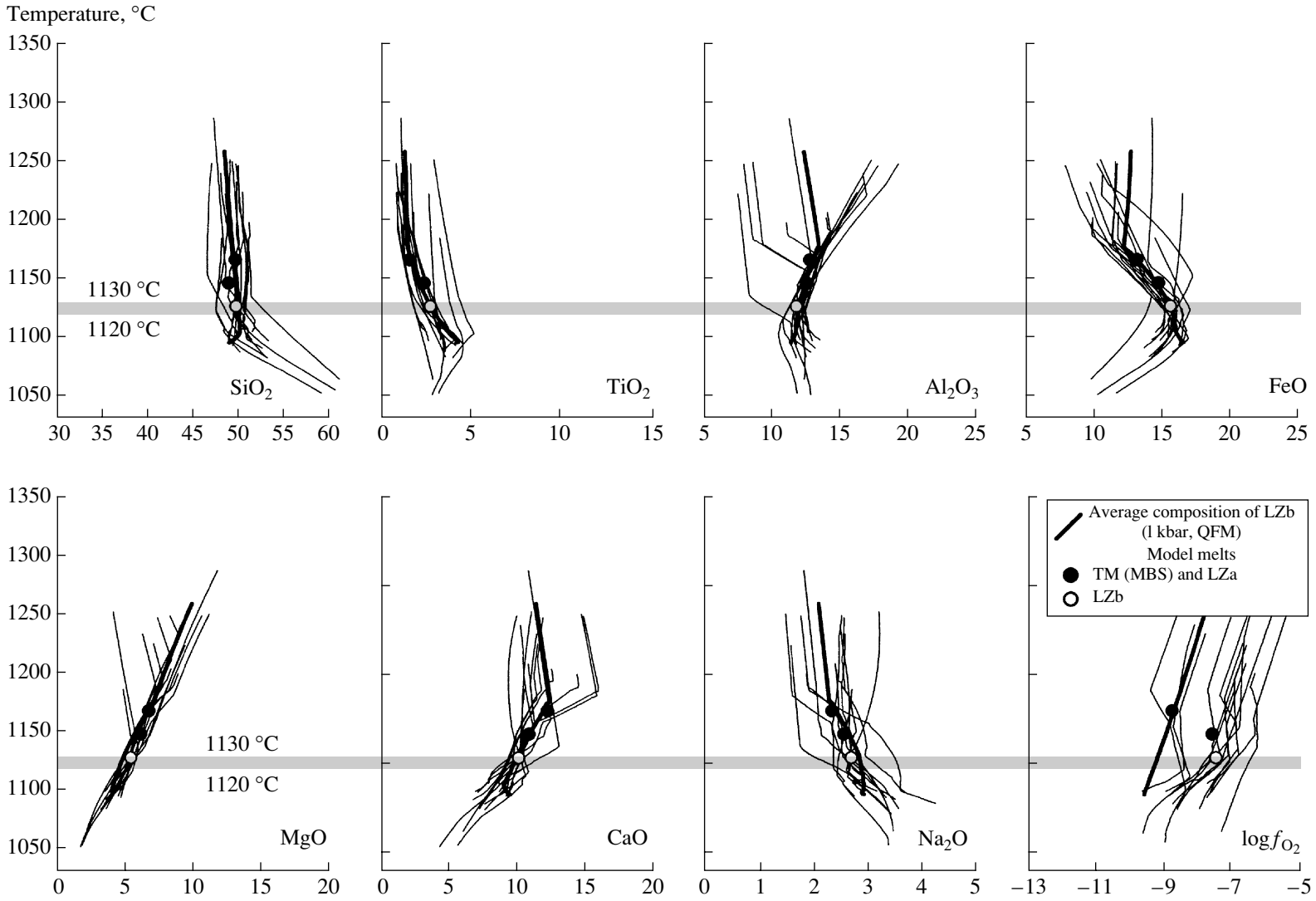

Fig. 7. Results of geochemical thermometry of the LZb zone.

Thin lines correspond to the trajectories of equilibrium crystallization calculated for the conditions closed with respect to oxygen. The temperature of 1125 ± 5°C is assumed to be the temperature of the primary *Ol–Pl–Aug* assemblage in equilibrium with intercumulus melt (see Table 3). Thick line represents the modeling results for the average composition of the LZb rocks (Table 2) under the QFM buffer conditions (Fig. 5). Compositions of the initial melts for the rocks of the Marginal Border Series (MBS) and LZa are shown for comparison.

Table 3. Thermodynamic parameters of the initial intercumulus melts and compositions of the primary cumulus minerals calculated for the main zones of the Layered Series

Components	LZa (n = 6)*	LZb (n = 14)	LZc (n = 9)	MZ (n = 17)	UZa (n = 8)
	1145** –7.5 ± 0.6***	1125 –7.4 ± 0.7	1100 –8.9 ± 0.4	1090 –9.8 ± 0.4	1085 –10.3 ± 0.6
Compositions of the intercumulus liquids, wt %					
SiO_2	49.26 ± 0.76	50.06 ± 1.25	48.04 ± 1.49	49.05 ± 0.86	50.31 ± 1.05
TiO_2	2.50 ± 0.58	2.83 ± 0.76	5.50 ± 0.63	5.25 ± 0.40	4.68 ± 0.24
Al_2O_3	12.74 ± 0.23	11.97 ± 0.77	10.26 ± 0.92	10.35 ± 0.90	11.05 ± 0.31
FeO	14.84 ± 0.81	15.73 ± 0.72	17.05 ± 0.73	17.50 ± 0.55	17.31 ± 0.58
MnO	0.20 ± 0.01	0.21 ± 0.04	0.22 ± 0.04	0.23 ± 0.04	0.24 ± 0.02
MgO	6.29 ± 0.23	5.56 ± 0.32	4.82 ± 0.26	4.00 ± 0.18	3.35 ± 0.19
CaO	11.02 ± 0.54	10.27 ± 0.59	11.00 ± 1.16	10.20 ± 0.78	9.01 ± 0.50
Na_2O	2.59 ± 0.32	2.73 ± 0.34	2.57 ± 0.34	2.80 ± 0.40	3.40 ± 0.29
K_2O	0.39 ± 0.07	0.42 ± 0.22	0.38 ± 0.17	0.39 ± 0.16	0.49 ± 0.14
P_2O_5	0.17 ± 0.06	0.22 ± 0.12	0.15 ± 0.06	0.21 ± 0.15	0.17 ± 0.06
Compositions of the equilibrium cumulus minerals, mol %					
Ol	*Fo* (74.9 ± 1.5)	*Fo* (72.1 ± 2.1)	*Fo* (64.0 ± 1.5)	See note	*Fo* (52.5 ± 2.5)
Pl	*An* (66.3 ± 1.9)	*An* (61.9 ± 2.1)	*An* (57.4 ± 2.1)	*An* (54.2 ± 2.9)	*An* (48.0 ± 3.1)
		En (47.0 ± 1.4)	*En* (42.2 ± 1.8)	*En* (39.5 ± 1.1)	*En* (38.0 ± 1.9)
Aug		*Fs* (13.6 ± 1.3)	*Fs* (16.8 ± 0.6)	*Fs* (20.2 ± 0.7)	*Fs* (22.6 ± 1.0)
		Wo (39.4 ± 0.9)	*Wo* (41.0 ± 1.7)	*Wo* (40.5 ± 1.0)	*Wo* (39.4 ± 1.2)
				En (54.3 ± 1.4)	*En* (51.4 ± 1.6)
Pig			See note	*Fs* (34.1 ± 1.5)	*Fs* (37.7 ± 1.4)
				Wo (11.6 ± 0.7)	*Wo* (10.9 ± 0.3)
Ilm			*Il* (91.4 ± 3.9)	*Il* (93.8 ± 2.8)	*Il* (93.7 ± 2.5)
Mt			*Ulv* (54.0 ± 6.6)	*Ulv* (72.3 ± 4.9)	*Ulv* (81.4 ± 6.7)

Note: All compositions are average compositions (±1σ) calculated at the point of the closest convergence and intersection of model trajectories, see Figs. 7 and 8. *Pig* existed in four cases in the LZc among the primary cumulus phases ($En_{59.1 \pm 0.9}Fs_{29.2 \pm 0.3}Wo_{11.7 \pm 0.9}$); 2–3 wt % *Ol* occurred in five cases in the MZ ($Fo_{56.6 \pm 1.4}$). *Il* and *Ulv* values characterize the $FeTiO_3$ and Fe_2TiO_4 activities calculated by equation from (Stormer, 1983).

* Zone or subzone; ** temperature, °C; *** log f_{O_2}.

Aug, *Pig*, *Ilm*, and *Mt*) compose various crystallization series or replace each other within a narrow temperature interval, actually within the accuracy of the COMAGMAT model (10–15°C). The most interesting result is that all of the samples devoid of modal olivine show *Ol* occurrence as a liquidus phase at the early and middle crystallization stages. Normally about 3–5 wt % of this mineral existed up to the system crystallinity of about 30%. Its proportion was up to 8–10 wt % in some cases. However, at 50–70% crystallinity, olivine was completely dissolved in reactions with pyroxene, oxides, and melt. Olivine was first to crystallize in eight cases at 1190–1160°C. The Fe–Ti oxides were first to crystallize also in eight cases. Four initial compositions were slightly oversaturated in plagioclase at 1210–1160°C. Augite was found at temperatures >1105°C in two cases, while pigeonite always crystallized at temperatures <1100°C. It is important that the low-Ca pyroxene appears at about 20–40% system crystallinity. This is consistent with the occurrence of this mineral among the primary cumulus phases, according to the petrographic subdivision of the Layered Series (Fig. 4). However, the main *Pig* volume (inverted at the later stages) probably formed by peritectic replacement of olivine.

The convergence of model trajectories of the MZ rock crystallization is as distinct as for the LZc rocks. The most dense clusters occur below 1100°C. The

problem is that the parallelism of the evolutionary lines for the multiphase assemblages at low temperatures precludes a precise determination of temperature and composition of the residual melt. We assume 1090°C to be the temperature of initial equilibrium, at which the model *Pl* composition (as a phase subjected to subsolidus re-equilibration at a lowest degree) is close to the natural compositions. The average composition of the trapped liquid calculated for 1090°C is shown in Fig. 8 and included in Table 3. As compared with the LZc composition, this melt is some richer in silica, iron, and alkalis and is complementarily depleted in TiO_2, MgO, and CaO. Note, that the TiO_2 decrease in melt may be related to *Ilm* and *Mt* separation in almost equal amounts. The model *Pl* composition ($An_{54.2 \pm 2.9}$) is close to the natural compositions (~An_{51}). The calculated pyroxene compositions are still more magnesian (Table 4). Ilmenite is still richer in $FeTiO_3$ at significantly higher ulvöspinel activity in titanomagnetite (Ulv_{72} in MZ against Ulv_{54} in LZc). This corresponds to a rapid decrease of the oxygen fugacity up to the log f_{O_2} values below the QFM buffer (Table 3, Fig. 8), which is consistent with estimates obtained during the independent studies (Williams, 1971; Morse *et al.*, 1980; Frost and Lindsley, 1992; McBirney, 1996).

The UZa subzone. The calculations of phase equilibria for ten UZa rocks yielded the lowest cotectic temperatures for the studied part of the Layered Series. No compositions with liquidus temperatures above 1200°C were found. The model crystallization sequences are similar to those calculated for the MZ. They begin with a short-term crystallization of single olivine or crystallization of the *Ol* + *Pl* ± oxides cotectic. Two samples with the highest FeO* contents (35 and 46 wt %) yielded the anomalously wide field of magnetite crystallization and were excluded from further consideration. Pyroxenes crystallized almost simultaneously at temperatures below 1100°C. The *Pig* stability field slightly decreased relative to the MZ rocks, which resulted in some increasing amount of modal olivine. The evolutionary lines of melts for the UZa form a dense cluster within the interval of 1090–1080°C. The average composition of this residual liquid at 1085°C has slightly elevated SiO_2 and FeO* concentrations (Table 3, Fig. 8). This melt can be considered as the most evolved derivative with the lowest MgO and CaO contents and elevated alkalinity. A slightly lower phosphorus concentration correlates with low P_2O_5 contents in the UZa rocks, which rarely exceed 0.1 wt % (McBirney, 1998). It is possible, however, that the assumed initial temperature of 1085°C is overestimated by 5–10°C, i. e., the density of the primary cumulus is somewhat underestimated, because of strong dependence of system crystallinity on temperature for the anchieutectic compositions. The decrease of temperature and amount of the trapped liquid should lead to elevated P_2O_5 concentrations in the residual melt, which are more consistent with the occurrence of abundant cumulus apatite in the overlying UZb (Fig. 4). The compositions of minerals of the initial six-phase assemblage continue the trend of depletion in refractory components from the underlying horizons (Table 3). Anorthite content in the model plagioclase ($An_{48.0 \pm 3.1}$) corresponds to the natural one (An_{46}), while the olivine composition is much more magnesian ($Fo_{52.5 \pm 2.5}$ against Fo_{40}). The calculated composition of Ca-pyroxene is 4–5 mol % richer in *Wo* as compared to the natural compositions, which is related to imperfect model of the augite solid solution in the COMAGMAT program. The ilmenite composition does not change, while magnetite has high Fe_2TiO_4 activity (0.81 ± 0.7) and actually moves to the ulvöspinel stability field. This is consistent with the tendency of rapid decrease of the oxygen fugacity in the lower part of the Upper Zone, $\log f_{O_2} = -10.3 \pm 0.6$ according to calculation for a closed system (Table 3, Fig. 8).

DISCUSSION

The geochemical thermometry data for the rocks of the Layered Series of the Skaergaard intrusion present a possible temperature interval of the melt trapped in intercumulus: about 60°C with variations of the initial temperatures from 1145 ± 10°C in the LZa to 1085 ± 10°C in the UZa. The interval of oxygen fugacity predetermined by the bulk composition of the residual liquid corresponds to $\log f_{O_2}$ decrease from the values exceeding QFM by 1–1.5 units in the LZa/LZb rocks to the QFM and lower values upsection from LZc. These parameters are consistent with data of other researchers (Lindsley *et al.*, 1969; Williams, 1971; Morse *et al.*, 1980; Frost *et al.*, 1988; Kersting *et al.*, 1989; Frost and Lindsley, 1992). The main result of the calculation consists in the estimation of the residual melt compositions, which can compose the general trend of the Skaergaard magma evolution (Table 3). This liquids show a strong enrichment in FeO* (up to ~18 wt %) and TiO_2 (up to ~5.5 wt %), and the corresponding trend is similar to the trend of evolution of the iron- and titanium-rich tholeiitic magmas, so-called Fe–Ti basalts (Brooks *et al.*, 1991). Such an interpretation is possible, but should be correlated with data on melts of rocks of the Marginal Border Series (Ariskin and Barmina, 2000) corresponding to the ordinary tholeiitic basalts (Table 1).

The results of geochemical thermometry do not support the conclusion (Wager and Brown, 1967) of the monotonous and long-term depletion of the residual melts in SiO_2 from the lower parts of the Lower Zone. Contrariwise, they demonstrate a slight increase of silica contents within the LZa (Fig. 7), which is consistent with experimental data on crystallization of the *Ol–Pl* assemblage in the tholeiitic systems (Grove and Baker, 1984; Ariskin and Barmina, 2000). The silica content in melt begin to decrease during the formation of the LZb

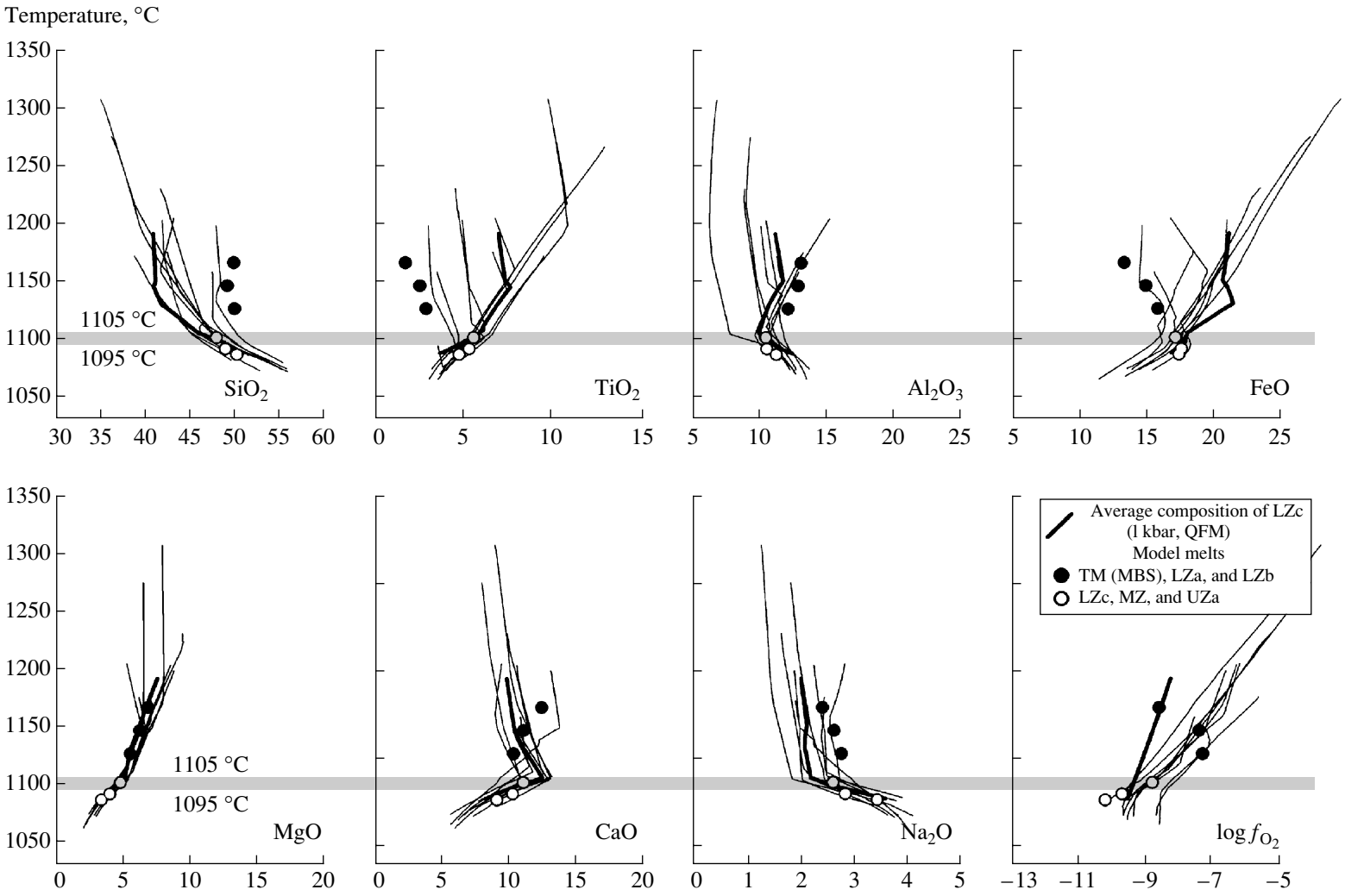

Fig. 8. Results of geochemical thermometry of the LZc subzone.

Thin lines correspond to the trajectories of equilibrium crystallization calculated for the conditions closed with respect to oxygen. The temperature of 1100 ± 5°C is assumed to be the temperature of the primary *Ol–Pl–Aug–Ilm–Mt* assemblage in equilibrium with intercumulus melt (see Table 3). Thick line represents the modeling results for the average composition of the LZc rocks (Table 2) under the QFM buffer conditions (Fig. 5). Compositions of the initial melts trapped in the rocks of the Marginal Border Series (MBS), as well as of the underlying and overlying horizons, are shown for comparison.

rocks due to separation of *Ol + Pl + Aug* assemblage, which leads to the relative low SiO_2 content for the melts of the overlying LZc rocks (Fig. 8, Table 3). However, this trend is rapidly changed by the trend of SiO_2 enrichment in intercumulus of the overlying horizons (in spite of the lower bulk silica contents in the rocks). The silica enrichment there is related to crystallization of abundant magnetite and ilmenite (*Ol + Pl + Aug* + oxides ± *Pig*). It is worth noting that the SiO_2 enrichment determined in the rocks from LZb to UZa is not as significant as it could be expected during the *Mt* crystallization in the systems with buffered f_{O_2} values. This correlates with insignificant FeO* variations (Table 3) that can be considered as evidence of the Skaergaard magma evolution under the conditions closed with respect to oxygen (Osborn, 1959; Presnall, 1966; Toplis and Carroll, 1996).

Note that the extraordinary decrease of the oxygen fugacity almost by three orders of magnitude in logarithmic units was observed within the temperature interval of 60°C (Table 3). This decrease cannot be accounted for only by evolution of the residual melts in the closed system. It is very strong and requires a partial openness of the system at the later stages of the intrusive chamber crystallization. However, such an oxygen fugacity cannot be maintained by any mineral buffer. These fugacity values could be caused by the influence of some reducing agent or fluid (probably, hydrogen-bearing), whose origin is a problem worthy of further studies.

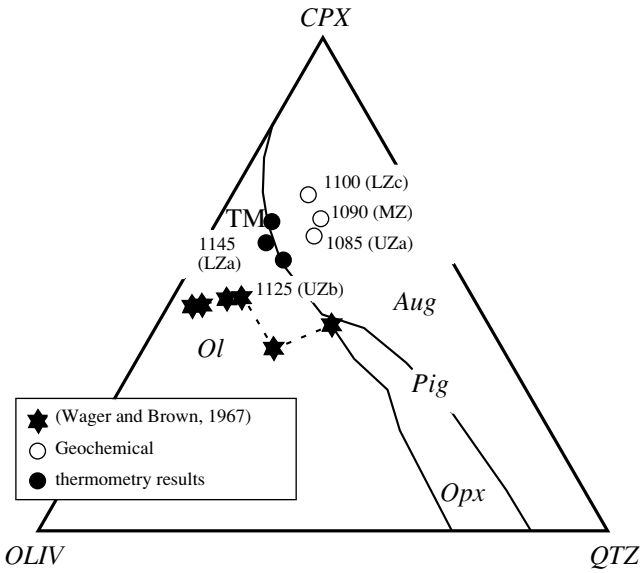

Fig. 9. Compositions of the residual melts by data of geochemical thermometry and classical series of the Skaergaard magma differentiates (Wager and Brown, 1967).

Model liquids are the initial composition for the rocks of the Marginal Border Series (TM, Table 1) and five compositions characterizing the intercumulus liquids in the main zones of the Layered Series (Table 3). The method of projection onto the *OLIV–CPX–QTZ* diagram (Grove and Baker, 1984; Tormey *et al.*, 1987) was modified in (Grove, 1993).

Possible Evidence of Compositional Convection

The most serious disagreement in the thermometric data is a distinct compositional gap between the melts of the LZa/LZb rocks and the melts representing the gabbroids rich in Fe–Ti oxides (from LZc to UZa) (Table 3). This is expressed in an abrupt "return" to the previous CaO and SiO_2 concentrations (Fig. 8), which can hardly be explained by the fractional crystallization of the parental magma. This disagreement could be ascribed to uncertainties in calculation by the COMAGMAT program and insufficient resolution of the method at low temperatures. Note, however, that the TiO_2 contents increase almost twice in the trapped liquid with the transition from LZb to LZc rocks. Such variations are much larger than the uncertainties of the used computer model (Ariskin and Barmina, 2000). In order to explain this fact based on the crystallization schemes we should assume a 40–50% crystallinity of the system and efficient redistribution of the strongly fractionated intercumulus liquids over the intrusive magma chamber. These speculations lead to the conclusion of the possible compositional convection in the initial mush of crystals and melt. This convection could be expressed in squeezing out and migration of interstitial liquid during the cumulus compaction and adcumulus growth of the primary crystals (Tait and Jaupart, 1992, 1996). Thus, the compositional gap attains a genetic meaning. It can be a geochemical indicator of the convection onset in the cumulus.

Artifact of the Wager's Calculations

The considered differences of the intercumulus melts become more contrasting, when their compositions are plotted in the *OLIV–CPX–QTZ* diagram proposed for interpretation of the low-pressure tholeiitic series (Fig. 9). This diagram was drawn using a large amount of experimental data for natural samples at an atmospheric pressure (Grove and Baker, 1984; Tormey *et al.*, 1987; Grove *et al.*, 1993). It demonstrates the well documented olivine–pyroxene phase boundaries corresponding to natural cotectics within the region of saturation in mafic minerals and plagioclase. This diagram shows the data points for six compositions calculated with geochemical thermometry including the initial composition TM of the contact rocks (Ariskin, 1999), as well as for a series of Skaergaard differentiates obtained by mass-balance calculations (Wager, 1960; Wager and Brown, 1967). It is obvious that the classical Wager's trend does not correspond to the experimental phase relations. Except for one point, the compositions are plotted within the *Ol–Pl* crystallization field and far away from the phase boundary corresponding to the appearance of high-Ca pyroxene. However, *Aug* occurs over the section as a main cumulus

Table 4. A comparison of Fe–Ti oxide proportions in the LZc by data of modal analysis and results of calculations using the COMAGMAT program for the system closed with respect to oxygen

Sample	LC-67	LC-342	LC-406	LC-534	LC-605	LC-727
Petrologic observations						
Bulk rock composition, wt %						
TiO_2	4.82	12.84	6.71	0.98	2.96	9.52
FeO	15.56	20.34	12.30	11.10	10.78	18.67
Fe_2O_3	5.63	10.31	4.80	1.41	4.21	11.46
Normative contents of Fe–Ti oxides, wt %						
Ilm	8.58	12.77	6.62	5.63	18.10	17.93
Mt	11.33	6.97	5.33	6.11	16.63	7.59
Modal contents of Fe–Ti oxides, wt %						
Ilm	4.5	23.1	12.7	0.9	3.5	13.0
Mt	13.5	8.2	4.0	2.2	5.2	23.7
Results of the computer modeling						
Phase relations, wt %						
System crystallinity, %	76.3	51.3	77.1	76.1	81.0	84.7
Ilm	2.6	21.2	9.5	0.0	1.4	14.5
Mt	12.3	8.9	7.0	1.0	6.7	21.9
Melt	23.7	48.7	22.9	23.9	19.0	15.3
Composition of the residual melt, wt %						
TiO_2	4.27	3.76	3.95	2.63	3.02	2.40
FeO	14.32	13.59	13.42	13.07	8.14	6.03
Fe_2O_3	3.10	4.62	2.76	3.86	3.57	2.31
Normative oxides in the residual melt, wt %						
Ilm	8.11	7.14	7.50	4.99	5.74	4.56
Mt	4.49	6.70	4.00	5.60	5.18	3.35
Bulk Fe–Ti oxide contents in the model rocks, wt %						
Ilm	4.5	24.7	11.2	1.2	2.5	15.2
Mt	13.4	12.2	7.9	2.3	7.7	22.4

Note: Normative contents of ilmenite and magnetite are calculated as pure components $FeTiO_3$ and F_3O_4 (CIPW). Modal mineral contents are determined by regression technique based on the bulk rock compositions and real mineral compositions (McBirney, 1998). Bulk Fe–Ti oxide contents in the model rocks were obtained as sums of the calculated phase proportions and normative contents of $FeTiO_3$ and Fe_3O_4 in the residual melts (multiplied by the melt fraction) at a given system crystallinity.

mineral from the middle part of the Lower Zone (Fig. 4). Only one composition of these differentiates falls within the real field of the *Ol–Pl–Aug–Pig* assemblage, because it is almost identical to the rocks of the Sandwich Horizon, which is considered to correspond to the final compositions of the residual liquid (Wager and Brown, 1967). The above consideration lead us to the conclusion that the classical trend with a strong FeO* enrichment and decreasing SiO_2 contents based on the relative proportions of the main structural units of the Layered Series (Fig. 1) is an artifact of the mass-balance calculations.

As to the data of geochemical thermometry, the first three highest temperature compositions (1165–1125°C) are confined precisely to the *Ol–Aug* boundary and form an evolutionary line directed to the pigeonite crystallization field. This trend corresponds to the early stages of the Skaergaard magma crystallization and is similar to the normal trend of the tholeiitic magma evolution (Ariskin *et al.*, 1987; Hunter and Sparks, 1987; Toplis and Carroll, 1996). The low-temperature melts of the LZc, MZ, and UZa rocks were found to be notably richer in normative diopside and form a series located above the *Ol–Aug–Pig* peritectic point. This

deviation from the phase boundaries is partly related to a strong enrichment in TiO_2 and the plotting technique on the *OLIV–CPX–QTZ* diagram, which is constructed by the data for the low-titanium systems (Grove, 1993). Nevertheless, a set of petrochemical differences (Table 3) and specific phase features (Fig. 9) indicate that the composition of the trapped liquid for the rocks enriched in Fe–Ti oxides deviates from the trends expected for the homogenous fractionation of the initial melt. Thus, these compositions also show some evidence of the superimposed processes or the processes complementary to the simple fractional crystallization. We could speculate that the infiltration of the intergranular liquid accompanied by some re-equilibration by the reaction with cumulus magnetite or ilmenite was the main factor of formation of the observed features of the residual melt composition.

The Problem of the Component Misbalance

The above consideration has raised one other issue, which was first discussed by Wager (1960). This is the inconsistence between the bulk composition of the Skaergaard intrusion and the possible initial magma composition. The calculation of the weighted average composition of the intrusion is complicated by the absence of precise data on volume proportions of the Layered, Upper Border, and Marginal Border series, but it is possible if the proportions are varied within certain reasonable limits. It is believed that the Layered Series comprises ~40–50% of the Skaergaard intrusion rocks, and the UBS and MBS proportions are nearly equal. This assumptions allow estimation of the bulk composition of the intrusion (A. McBirney, personal communication). One of these model compositions are given in Table 1, where it is compared with compositions of chilled gabbro and initial liquids. It is obvious that the observed average TiO_2 and P_2O_5 contents are several times higher than those in any proposed parental magma. The intrusion is by about 3 wt % lower in silica and is richer in iron. This result does not seem extraordinary, because the *Mt–Ilm* cumulates dominate the studied part of the Layered Series (Fig. 3). The closeness of the system suggests two explanations for these discrepancies. The first one is based on the assumption that the whole section (unavailable to direct observation) of the Layered Series contains more silica and less iron and titanium oxides. This requires the existence of the Hidden Layered Series composing no less than 65% of the whole section (Wager, 1960; Wager and Brown, 1967). Another interpretation postulates the formation of relatively acid differentiates, the main part of which was removed by erosion of the Upper Border Series (Hunter and Sparks, 1987).

The results of our calculations demonstrate that the compositional differences between the melts entrapped in the contact rocks (TM, Table 1) and gabbroids of the Lower Zone (LZa, Table 3) are small. In this case the Hidden Layered Series is not necessary, if the initial magma was homogenous. If the parental magma was heterogeneous and entrained into the intrusive chamber >40–50% crystals (*Ol* + *Pl*) equilibrated with the TM-type melt (Ariskin, 1999), then the complementary volume of troctolite cumulates should be suggested to exist at a depth, in spite of the data indicating the absence of any thick hidden zone (Blank and Gettings, 1973; McBirney, 1975).

Thus, the problem of general compositional misbalance of the Skaergaard intrusion is the geologic, rather than petrologic problem. Let us note in this context that the rocks similar to the *Mt–Ilm* cumulates of the Skaergaard intrusion compose ~10% of the Layered Series of the Kiglapait intrusion. This intrusion is about 9 km thick and is composed of about 85% troctolites (Morse, 1981). The data on geochemical thermometry of the contact rocks of this intrusion and weighted average composition of the Layered Series indicate that the Kiglapait magma was heterogeneous containing about 25% intratelluric *Ol* and *Pl* crystals (Barmina and Ariskin, 2002). Like in the Skaergaard intrusion, only relics of the Upper Border Series occur in the Kiglapait intrusion. The results of the thermometric calculations for the rocks of the lower horizons yield the melts that are notably poorer in TiO_2 and P_2O_5 than the liquid calculated using the composition of the Layered Series.

These observations also raise the question on the possibility and scale of occurrence of the intermediate and acid differentiates in the Skaergaard intrusion. The laws of phase equilibria suggest an inevitable silica enrichment in the residual magmas during crystallization of the Fe–Ti oxides. However, the geologic data do not verify the existence of comparable amount of more siliceous rocks. This contradiction occurs together with the general misbalance in the FeO* and SiO_2 distribution (see above). The existence of the silica-rich differentiates cannot be proved or disproved in this case. Two facts seem important in this context. First, the Upper Zone of the Layered Series and the Upper Border Series typically includes the segregational veins and pockets of granophyres containing from 55 to 70 wt % SiO_2 (McBirney, 1989). Second, the appearance of *Pig* in the crystallization sequence indicates an elevated silica activity in liquid. Together with the data on modeling of the crystallization trajectories for individual rocks (Figs. 7, 8), this is a serious argument for the former existence of the relatively acid residual melts (>50% SiO_2), which could be trapped *in situ* as the intercumulus liquid. It is possible that some portions of this low-density interstitial liquid could migrate to the overlying horizons and undergo further fractionation up to the complete removal of Mg from the melt, as it is observed in the Sandwich Horizon. However, this suggestion does not solve the general misbalance problem.

CONCLUSION

The calculations using the geochemical thermometry for the rocks of the Layered Series of the Skaergaard

intrusion are the first attempts of comprehensive genetic interpretation of the structure of this intrusion based on computer modeling of the primary phase equilibria. The present results are preliminary in many respects, and most estimates strongly depend on the precision of the applied COMAGMAT model. The experience of such calculations shows that, even though the error in estimation of the equilibrium temperature is ±10°C, it is difficult to obtain a univocal solution for the assemblages comprising five–six mineral phases and melt. Nevertheless, the obtained values of temperature, intrinsic oxygen fugacity, and element concentrations in the residual liquids (Table 3) are in good agreement with data of petrologic observations and independent thermodynamic calculations and are consistent with the general scheme of the Layered Series structure. Thus, the geochemical thermometry is the most self-consistent method for interpretation of the intrusive basic rock crystallization. This method is devoid of many drawbacks, which are typical of the simple mass-balance calculations. This statement is illustrated by inconsistence of the classical Wager's trend to the crystallization laws of the ferrobasaltic systems (Figs. 1, 9). This series of the Skaergaard melts (reported and cited in many petrologic and educational publications) should be considered as a rather rough approximation of the natural evolutionary line, which only demonstrates the general features of the basaltic magma fractionation (MgO decrease, FeO* and P_2O_5 increase, etc.). This conclusion is no detraction from Wager and his colleagues' merits, who made a great contribution to understanding the intrusive magma chamber differentiation. The modern knowledge of the natural phase relationships and development of modeling of the phase equilibria allowed us to extend the potentials of their approaches and introduce more physicochemical meaning into the final results.

ACKNOWLEDGMENTS

The author is grateful to Academician V.A. Zharikov (Institute of Experimental Mineralogy, Russian Academy of Sciences) for his suggestion to contribute the preparation of this journal issue. I thank Prof. A.R. McBirney, who initiated the geochemical thermometry of the Skaergaard rocks, provided numerous petrochemical data, and made some valuable remarks during the discussion of the results. The meaningful comments of E.V. Koptev-Dvornikov (Moscow State University) made the final version of the paper more explicit.

The study was supported by the Russian Foundation for Basic Research, project no. 02-05-64118, and by the Foundation for the Advancement of Russian Science.

REFERENCES

Ariskin, A.A. and Barmina, G.S., *Modelirovanie fazovykh ravnovesii pri kristallizatsii bazal'tovykh magm* (Simulation of Phase Equilibria during Basaltic Magmas Crystallization), Moscow: Nauka, 2000.

Ariskin, A.A. and Barmina, G.S., An Empirical Model for the Calculation of Spinel–Melt Equilibrium in Mafic Igneous Systems at Atmospheric Pressure: II. Fe–Ti Oxides, *Contrib. Mineral. Petrol.*, 1999, vol. 134, pp. 251–263.

Ariskin, A.A., Barmina, G.S., Frenkel, M.Ya., and Yaroshevskii, A.A., Computer Simulation of Fractional Crystallization of Tholeiitic Magmas under a Low Pressure, *Geokhimiya*, 1987, no. 9, pp. 1240–1259.

Ariskin, A.A., Frenkel, M.Ya., Barmina, G.S., and Nielsen, R.L., COMAGMAT: A Fortran Program to Model Magma Differentiation Processes, *Comput. Geosci.*, 1993, vol. 19, pp. 1155–1170.

Ariskin, A.A., Konnikov, E.G., and Kislov, E.V., Simulation of Equilibrium Crystallization of Ultramafic Rocks as Applied to the Development of Phase Layering of the Dovyren Pluton, Northern Baikal Area, Russia, *Geokhimiya*, 2002 (in press).

Ariskin, A.A., Phase Equilibria Modeling in Igneous Petrology: Use of COMAGMAT Model for Simulating Fractionation of Ferrobasaltic Magmas and the Genesis of High-Alumina Basalt, *J. Volcanol. Geotherm. Res.*, 1999, vol. 90, pp. 115–162.

Ariskin, A.A., Calculation of Titanomagnetite Stability at the Liquidus of Basalts and Andesites with Special Reference to the Differentiation of Tholeiitic Magmas, *Geokhimiya*, 1998, no. 1, pp. 18–27.

Barmina, G.S., Ariskin, A.A., and Frenkel, M.Ya., Petrochemical Types and Crystallization Conditions of Plagiodolerites from the Kronotskii Peninsula, Eastern Kamchatka, *Geokhimiya*, 1989, no. 2, pp. 192–206.

Barmina, G.S. and Ariskin, A.A., Estimation of the Chemical and Phase Characteristics of Initial Magma of the Kiglapait Troctolite Intrusion, Labrador, Canada, *Geokhimiya*, 2002 (in press).

Barmina, G.S., Ariskin, A.A., Koptev-Dvornikov, E.V., and Frenkel, M.Ya., Estimation of the Composition of Primary Cumulative Minerals from Differentiated Traps, *Geokhimiya*, 1988, no. 8, pp. 1108–1119.

Blank, H.R. and Gettings, M.E., Subsurface Form and Extent of the Skaergaard Intrusion, East Greenland, *Trans. Am. Geophys. Union*, 1973, vol. 54, p. 507.

Brooks, C.K. and Nielsen, T.F.D., Early Stages in the Differentiation of the Skaergaard Magma as Revealed by a Closely Related Suite of Dike Rocks, *Lithos*, 1978, vol. 11, pp. 1–14.

Brooks, C.K. and Nielsen, T.F.D., The Differentiation of the Skaergaard Intrusion. A Discussion of Hunter and Sparks (Contrib. Mineral. Petrol. 95: 451–461), *Contrib. Mineral. Petrol.*, 1990, vol. 104, pp. 244–247.

Brooks, C.K., Larsen, L.M., and Nielsen, T.F.D., Importance of Iron-Rich Tholeiitic Magmas at Divergent Plate Margins: A Reappraisal, *Geology*, 1991, vol. 19, pp. 269–272.

Carmichael, I.S.E., The Petrology of Thingmuli, a Tertiary Volcano in Eastern Island, *J. Petrol.*, 1964, vol. 5, pp. 435–460.

Chalokwu, C.I., Grant, N.K., Ariskin, A.A., and Barmina, G.S., Simulation of Primary Phase Relations and Mineral Compositions in the Partridge River Intrusion, Duluth Complex,

Minnesota: Implications for the Parent Magma Composition, *Contrib. Mineral. Petrol.*, 1993, vol. 114, pp. 539–549.

Frenkel, M.Ya., Ariskin, A.A., Barmina, G.S., *et al.*, Geochemical Thermometry of Igneous Rocks: Principles and Examples, *Geokhimiya*, 1987, no. 11, pp. 1546–1562.

Frenkel, M.Ya., Yaroshevskii, A.A., Ariskin, A.A., *et al.*, *Dinamika vnutrikamernoi differetsiatsii bazitovykh magm* (The Dynamics of *in situ* Differentiation of Mafic Magmas), Moscow: Nauka, 1988.

Frenkel, M.Ya., Yaroshevskii, A.A., Koptev-Dvornikov, E.V., *et al.*, Crystallization Mechanism of Layering Development in Sheet-Shaped Intrusions, *Zap. Vses. Mineral. O–va*, 1985, vol. 104, no. 3, pp. 257–274.

Frost, B.R., Lindsley, D.H., and Anderson, D.J., Fe–Ti Oxide–Silicate Equilibria: Assemblages with Fayalitic Olivine, *Am. Mineral.*, 1988, vol. 73, pp. 727–740.

Frost, B.R. and Lindsley, D.H., Equilibria among Fe–Ti Oxides, Pyroxenes, Olivine, and Quartz: Part II. Application, *Am. Mineral.*, 1992, vol. 77, pp. 1004–1020.

Ghiorso, M.S. and Carmichael, I.S.E., Chemical Mass Transfer in Magmatic Processes. II. Applications in Equilibrium Crystallization, Fractionation and Assimilation, *Contrib. Mineral. Petrol.*, 1985, vol. 90, pp. 121–141.

Grove, T.L. and Baker, M.B., Phase Equilibrium Controls on the Tholeiitic Versus Calc–Alkaline Differentiation Trends, *J. Geophys. Res.*, 1984, vol. 89B, pp. 3253–3274.

Grove, T.L., Corrections to Expressions for Calculating Mineral Components in "Origin of Calc–Alkaline Series Lavas at Medicine Lake Volcano by Fractionation, Assimilation, and Mixing" and "Experimental Petrology of Normal MORB near the Kane Fracture Zone: 22°–25°N, Mid-Atlantic Ridge," *Contrib. Mineral. Petrol.*, 1993, vol. 114, pp. 422–424.

Hoover, J.D., The Chilled Marginal Gabbro and Other Contact Rocks of the Skaergaard Intrusion, *J. Petrol.*, 1989, vol. 30, pp. 441–476.

Hunter, R.H. and Sparks, R.S.J., The Differentiation of the Skaergaard Intrusion, *Contrib. Mineral. Petrol.*, 1987, vol. 95, pp. 451–461.

Hunter, R.H. and Sparks, R.S.J., The Differentiation of the Skaergaard Intrusion. Replies to A.R. McBirney and H.R. Naslund, to S.A. Morse, to C.K. Brooks and T.F.D. Nielsen, *Contrib. Mineral. Petrol.*, 1990, vol. 104, pp. 248–254.

Jang, Y.D. and Naslund, H.R., Major and Trace Element Composition of Skaergaard Plagioclase; Geochemical Evidence for Changes in Magma Dynamics during the Final Stage of Crystallization of the Skaergaard Intrusion, *Contrib. Mineral. Petrol.*, 2001, vol. 140, pp. 441–457.

Kersting, A.B., Arculus, R.J., Delano, J.W., and Loureiro, D., Electrochemical Measurements Bearing on the Oxidation State of the Skaergaard Layered Intrusion, *Contrib. Mineral. Petrol.*, 1989, vol. 102, pp. 376–388.

Krivolutskaya, N.A., Ariskin, A.A., Sluzhenkin, S.F., and Turovtsev, D.M., Geochemical Thermometry of the Talnakh Intrusion: Assessment of the Melt Composition and Crystallinity of Parental Magma, *Petrologiya*, 2001, vol. 9, no. 5, pp. 451–479.

Lindsley, D.H., Brown, G.M., and Muir, I.D. Conditions of the Ferrowollastonite–Ferrohedenbergite Inversion in the Skaergaard Intrusion, East Greenland, *Mineral. Soc. Am. Spec. Publ.*, 1969, vol. 2, pp. 193–201.

McBirney, A.R. and Nakamura, Y., Immiscibility in Late Stage of the Skaergaard Intrusion, *Carnegie Inst. Wash. Yb.*, 1973, vol. 72, pp. 348–352.

McBirney, A.R. and Naslund, H.R., The Differentiation of the Skaergaard Intrusion. A Discussion of Hunter and Sparks (Contrib. Mineral. Petrol. 95: 451–461), *Contrib. Mineral. Petrol.*, 1990, vol. 104, pp. 235–240.

McBirney, A.R., Differentiation of the Skaergaard Intrusion, *Nature*, 1975, vol. 253, pp. 691–694.

McBirney, A.R., The Skaergaard Intrusion, in *Layered Intrusions*, Cawthorn, R.G., Ed., Amsterdam: Elsevier, 1996, pp. 147–180.

McBirney, A.R., The Skaergaard Layered Series: I. Structure and Average Compositions, *J. Petrol.*, 1989, vol. 30, pp. 363–397.

McBirney, A.R., The Skaergaard Layered Series: Part V. Included Trace Elements, *J. Petrol.*, 1998, vol. 39, pp. 255–276.

Morse, S.A., Kiglapait Geochemistry. IV: The Major Elements, *Geochim. Cosmochim. Acta*, 1981, vol. 45, pp. 461–479.

Morse, S.A., Lindsley, D.H., and Williams, R.J., Concerning Intensive Parameters in the Skaergaard Intrusion, *Am. J. Sci.*, 1980, vol. 280A, pp. 159–170.

Naslund, H.R. and McBirney, A.R., Mechanisms of Formation of Igneous Layering, in *Layered Intrusions*, Cawthorn, R.G., Ed., Amsterdam: Elsevier, 1996, pp. 1–43.

Nikolaev, G.S., Borisov, A.A., and Ariskin, A.A., New f_{O_2} Barometers for Quenched Glasses of Various Petrochemical Series, *Geokhimiya*, 1996, no. 9, pp. 836–839.

Osborn, E.F., Role of Oxygen Pressure in the Crystallization and Differentiation of Basaltic Magma, *Am. J. Sci.*, 1959, vol. 257, pp. 609–647.

Presnall, D.C., The Join Forsterite–Diopside–Iron Oxide and Its Bearing on the Crystallization of Basaltic and Ultramafic Magmas, *Am. J. Sci.*, 1966, vol. 264, pp. 753–809.

Sack, R.O., Carmichael, I.S.E., Rivers, M., and Ghiorso, M.S., Ferric–Ferrous Equilibria in Natural Silicate Liquids at 1 bar, *Contrib. Mineral. Petrol.*, 1980, vol. 75, pp. 369–376.

Sato, M. and Valenza, M., Oxygen Fugacities of the Layered Series of the Skaergaard Intrusion, East Greenland, *Am. J. Sci.*, 1980, vol. 280A, pp. 134–158.

Sharapov, V.N., Cherepanov, A.N., Popov, V.N., and Lobov, A.G., Dynamics of Basite Melt Cooling during Filling of Funnel-Shaped Intrusion Chamber, *Petrologiya*, 1997, vol. 5, no. 1, pp. 10–22.

Snyder, D., Carmichael, I.S.E., and Wiebe, R.A., Experimental Study of Liquid Evolution in a Fe-Rich, Layered Mafic Intrusion: Constraints of the Fe–Ti Oxide Precipitation on the Ti–f_{O_2} and Ti–ρ Paths of Tholeiitic Magmas, *Contrib. Mineral. Petrol.*, 1993, vol. 113, pp. 73–86.

Stormer, J.C., Jr., The Effects of Recalculation on Estimates of Temperature and Oxygen Fugacity from Analyses of Multicomponent Iron–Titanium Oxides, *Am. Mineral.*, 1983, vol. 68, pp. 586–594.

Tait, S. and Jaupart, C., Compositional Convection in a Reactive Crystalline Mush and Melt Differentiation, *J. Geophys. Res.*, 1992, vol. 97, pp. 6735–6756.

Tait, S. and Jaupart, C., The Production of Chemically Stratified and Accumulate Plutonic Igneous Rocks, *Mineral. Mag.*, 1996, vol. 60, pp. 99–114.

Tegner, C., Iron in Plagioclase as a Monitor of the Differentiation of the Skaergaard Intrusion, *Contrib. Mineral. Petrol.*, 1997, vol. 128, pp. 45–51.

Toplis, M.J. and Carroll, M.R., An Experimental Study of the Influence of Oxygen Fugacity on Fe–Ti Oxide Stability, Phase Relations, and Mineral–Melt Equilibria in Ferrobasaltic Systems, *J. Petrol.*, 1995, vol. 36, pp. 1137–1170.

Toplis, M.J. and Carroll, M.R., Differentiation of Ferrobasaltic Magmas under Conditions Open and Closed to Oxygen: Implications for Skaergaard Intrusion and Other Natural Systems, *J. Petrol*., 1996, vol. 37, pp. 837–858.

Tormey, D.R., Grove, T.L., and Bryan, W.B., Experimental Petrology of Normal MORB Near the Kane Fracture Zone: 22°–25°N, Mid-Atlantic Ridge, *Contrib. Mineral. Petrol.*, 1987, vol. 96, pp. 121–139.

Wager, L.R. and Brown, G.M., *Layered Igneous Rocks*, Edinburgh: Oliver and Boyd, 1967.

Wager, L.R. and Deer, W.A., Geological Investigations in East Greenland, Part III. The Petrology of the Skaergaard Intrusion, Kangerdlugssuaq, East Greenland, *Meddelelser om Gronland*, 1939, vol. 105, pp. 1–352.

Wager, L.R., The Major Element Variation of the Layered Series of the Skaergaard Intrusion and Reestimation of the Average Composition of the Hidden Layered Series and of the Successive Residual Magmas, *J. Petrol.*, 1960, vol. 1, pp. 364–398.

Williams, R.J., Reaction Constants in the System FeO–MgO–SiO_2–O_2; Intensive Parameters in the Skaergaard Intrusion, East Greenland, *Am. J. Sci.*, 1971, vol. 271, pp. 132–146.